

# Bacterial Community in Saline Farmland Soil on the Tibetan Plateau: Responding to Salinization While Resisting Extreme Environments

**Yiqiang Li**

School of Ocean Sciences, China University of Geosciences (Beijing), Beijing, 100083, China

**XUsheng Wang**

School of Ocean Sciences, China University of Geosciences (Beijing), Beijing, 100083, China

**Yinghui Chai**

Laboratory division, Eighth Medical Center of Chinese People's Liberation Army General Hospital, Beijing 100000, PR China

**Liying Huang**

Institute of Agricultural Quality Standards and Testing, Tibet Academy of Agriculture and Animal Husbandry Sciences, 850000, China

**Ximing Luo**

Beijing Key Laboratory of Water Resources and Environmental Engineering, China University of Geosciences (Beijing), Beijing, 100083, China

**Cheng Qiu**

Institute of Agricultural Quality Standards and Testing, Tibet Academy of Agriculture and Animal Husbandry Sciences, 850000, China

**Qinghai Liu**

Institute of Agricultural Quality Standards and Testing, Tibet Academy of Agriculture and Animal Husbandry Sciences, 850000, China

**Xiangyu Guan** (✉ [guanxy@cugb.edu.cn](mailto:guanxy@cugb.edu.cn))

Beijing Key Laboratory of Water Resources and Environmental Engineering, China University of Geosciences (Beijing), Beijing, 100083, China

---

## Research Article

**Keywords:** Saline, Tibetan Plateau, Metagenomics, Microbial community, Resistance mechanism

**Posted Date:** January 20th, 2021

**DOI:** <https://doi.org/10.21203/rs.3.rs-140957/v1>

**License:**  This work is licensed under a Creative Commons Attribution 4.0 International License.

[Read Full License](#)

---

**Version of Record:** A version of this preprint was published at BMC Microbiology on April 20th, 2021. See the published version at <https://doi.org/10.1186/s12866-021-02190-6>.

1 **Bacterial community in saline farmland soil on the Tibetan Plateau:**  
2 **Responding to salinization while resisting extreme environments**

3 YiQiang Li<sup>1</sup>, YingHui Chai<sup>1,2</sup>, XuSheng Wang<sup>1</sup>, LiYing Huang<sup>3</sup>, XiMing Luo<sup>1,4</sup>,  
4 Cheng Qiu<sup>3</sup>, QingHai Liu<sup>3</sup>, XiangYu Guan<sup>1,4,\*</sup>

5

6 <sup>1</sup> School of Ocean Sciences, China University of Geosciences (Beijing), Beijing,  
7 100083, China

8 <sup>2</sup> Laboratory division, Eighth Medical Center of Chinese People's Liberation Army  
9 General Hospital, Beijing100000, PR China

10 <sup>3</sup> Institute of Agricultural Quality Standards and Testing, Tibet Academy of  
11 Agriculture and Animal Husbandry Sciences,850000, China

12 <sup>4</sup> Beijing Key Laboratory of Water Resources and Environmental Engineering, China  
13 University of Geosciences (Beijing), Beijing, 100083, China

14

15 \* **Corresponding author:** School of Ocean Sciences, China University of  
16 Geosciences (Beijing), Beijing, 100083, China. E-mail address: guanxy@cugb.edu.cn  
17 (X. Guan).

18

19

## 20 **Abstract**

21 **Background:** Soil salinization caused by irrigation will reduce soil health and  
22 crop yields. Soil salinization has become one of the world's soil degradation problems.  
23 There are few studies on the response of microbial communities to soil salinization in  
24 plateau environments. Here, we applied metagenomics technology to make an  
25 exploration on the salinized soil microorganisms of the Tibetan Plateau.

26 **Results:** The metagenomic data results show that the microbial species diversity  
27 and genome diversity of saline soil and non-saline soil have changed significantly. we  
28 found that the abundances of chemoautotrophic and acidophilic bacteria comprising  
29 *Rhodanobacter*, *Acidobacterium*, *Candidatus Nitrosotalea*, and *Candidatus*  
30 *Koribacter* were significantly higher in saline soil. and the potential degradation of  
31 organic carbon in saline soil. The potential degradation of organic carbon in the saline  
32 soil, as well as the production of NO and N<sub>2</sub>O via denitrification, and the production  
33 of sulfate by sulfur oxidation were significantly higher compared with the non-saline  
34 soil. Both types of soils were rich in genes encoding resistance to environmental  
35 stresses (i.e., cold, ultraviolet light, and hypoxia). The resistance of the soil microbial  
36 communities to the saline environment on the Tibetan Plateau is based on the  
37 absorption of K<sup>+</sup> as the main mechanism, with cross-protection proteins and  
38 absorption buffer molecules as auxiliary mechanisms. Network analysis showed that  
39 functional group comprising chemoautotrophic and acidophilic bacteria had  
40 significant positive correlations with electrical conductivity and total sulfur, and

41 significant negative correlations with the total organic carbon, pH, and available  
42 nitrogen. The soil moisture, pH, and electrical conductivity are likely to affect the  
43 bacterial carbon, nitrogen, and sulfur cycles.

44 **Conclusions:** These results indicate that the specific environment of the Tibetan  
45 Plateau and salinization jointly shape the structure and function of the soil bacterial  
46 community, and that the bacterial communities respond to complex and harsh living  
47 conditions. In addition, environmental feedback probably exacerbates greenhouse gas  
48 emissions and accelerates the reduction in the soil pH. This study will provide insights  
49 into the microbial response to soil salinization and the potential ecological risks for  
50 the special plateau environment.

51 **Keywords:** Saline, Tibetan Plateau, Metagenomics, Microbial community, Resistance  
52 mechanism

## 53 **Background**

54 The Tibetan Plateau is located at a high altitude (average > 4,500 m), with severe cold  
55 and low oxygen levels, and it is strongly affected by ultraviolet radiation [1, 2]. Due  
56 to global warming, population increases, and the fragility of the Tibetan Plateau  
57 environment, various ecological and environmental problems have occurred, such as  
58 vegetation degradation, biodiversity decline, desertification, and salinization [3, 4].  
59 Soil is the basis of the function of the global terrestrial ecosystem [5] and soil  
60 salinization is considered one of the most pressing environmental challenges for the

61 world [6, 7]. The continued salinization of scarce agricultural soil resources will have  
62 feedback effects on global climate change, as well as detrimentally affecting the  
63 already poor living conditions for people on the Tibetan Plateau. However, the  
64 problem of saline soil and its environmental impact in the context of extreme climate  
65 change in this complex and fragile environment have received little attention.

66 Soil microorganisms are essential components of the soil ecosystem on the  
67 Tibetan Plateau and they play key roles in the health of the ecosystem [8, 9]. Soil  
68 microorganisms are involved in the conversion of most nutrients in the soil, and they  
69 have critical roles in the decomposition and stabilization of soil organic matter and the  
70 nutrient cycle, thereby influencing plant growth and the productivity of aboveground  
71 plants [10, 11]. High salinity has adverse effects on biological activities. The  
72 microbial community will adapt to changes in salinity by adjusting its composition  
73 and enhancing interactions [12, 13]. Microorganisms adapt to high salinity  
74 environment mainly through two mechanisms comprising the synthesis or absorption  
75 of organic osmotic agents, and absorbing  $K^+$  and other inorganic ions to resist osmotic  
76 stress [14, 15], thereby maintaining the normal life activities of cells under high  
77 osmotic pressure conditions. Soil samples from different high salinity regions vary  
78 greatly in microbial community structures, and bacteria are more sensitive than fungi  
79 [16, 17]. In-depth investigations of changes in the structure and function of bacterial  
80 communities as sensitive factors will help us to understand the mechanisms  
81 responsible for maintaining the function of saline soil ecosystems.

82 Studies of saline soils throughout the world have shown that salinity has  
83 important effects on the microbial community composition and metabolic functions.  
84 Salinity leads to significant decreases in the soil microbial diversity and biomass,  
85 reductions in the soil enzyme activities [18, 19], inhibition of bacterial growth and  
86 respiration [20], retardation of the organic matter degradation rate and suppression of  
87 nitrification [21]. The mechanisms of bacteria resisting high salinity environments  
88 consume large amounts of energy, and the organic matter in the soil will be consumed  
89 rapidly [22]. Bacteria with autotrophic capacities have survival advantages in a  
90 nutrient-poor environment, thereby leading to changes in the metabolic functional  
91 network for the bacterial community. However, no bacteria are specifically adapted to  
92 high-salinity soil environments and it is not easy to find bacterial indicator in salinity  
93 soil [23]. The soil microbial community on the Tibetan Plateau has responded to  
94 extreme environmental pressures via a unique metabolic mechanism [24, 25].  
95 However, the microbial communities in saline soils at high altitude have not been  
96 investigated.

97 In the 6<sup>th</sup> century BC, humans mainly settled in the northeast area of the Tibetan  
98 Plateau, and they did not extend their agricultural activities to the land higher than  
99 3600 meters above sea level in the central and southern Tibetan Plateau until 3500 cal  
100 yr B.P [26]. The melting of glaciers and repeated freezing–thawing of permanently  
101 frozen soils caused by global warming have partially exposed the glacier-covered  
102 mineralized rock layers on the surface of the Tibetan Plateau. In addition, the

103 increased water yield has accelerated the leaching of various minerals in the rock and  
104 acid rock drainage into the rivers [27, 28]. Thus, irrigation using river water has  
105 resulted in large amounts of sulfate and metal ions being applied to land, leading to  
106 salinization of the soil in the study area. The environmental challenges encountered  
107 by soil bacterial communities in farmland in the study area include high soil salinity,  
108 temperature differences between the day and night, extremely strong ultraviolet  
109 radiation, limited oxygen, and other extreme conditions. Thus, bacterial survival  
110 under these conditions evolved specific survival strategies. In this study, we will focus  
111 on the: (1) characteristics of bacterial community in saline soil on the Tibetan Plateau,  
112 and their biogeochemical cycling processes, (2) the mechanisms associated with the  
113 responses to multiple environmental pressures, and (3) the potential impacts of  
114 bacterial communities in salinized soil on environmental climate.

## 115 **Methods**

### 116 **Soil sampling**

117 The study area is located in Naidong County, Shannan City, Tibet, with an average  
118 altitude of 3560 m. Yala Snow Mountain is a natural snow mountain glacier with the  
119 highest altitude in the area of 6647 m and it is the main water source. The study area  
120 has a temperate monsoon plateau climate and the air is thin. The average annual  
121 temperature in Naidong County is 8.8°C, the average annual pressure is 660.4 hPa,

122 the average annual solar radiation is 6018.9 MJ, and the average annual precipitation  
123 is 383.2 mm.

124 In May 2019, saline soil samples (SA) were collected from farmland near the  
125 Zhiqu River that had been planted with barley (Fig. S1), and nonsaline soil samples  
126 (CK) were collected as a control from farmland near the Yalong River (Xiangqu) that  
127 had also been planted with barley. Five subsamples were collected at each sampling  
128 site according to the four corners of a square and the center point, where the side  
129 length was about 10 m. The surface 5–20 cm soil layer was collected and each sample  
130 was packed in a 50-ml sterile centrifuge tube. The sample tubes were refrigerated with  
131 ice packs and returned to the laboratory within 24 hours. Each of the subsamples was  
132 passed through a 2-mm sieve in the laboratory to remove any stones and plant debris.  
133 The five soil subsamples from the same location were mixed to obtain one sample.  
134 The mixed saline soil samples were designated as S1, S2, S3, S4, S5, and S6, and the  
135 nonsaline soil samples as N1, N2, N3, N4, N5, and N6. Each soil sample was divided  
136 into two parts, and one was stored at 4°C for subsequent chemical tests and  
137 experiments in the laboratory. The other was kept at –20°C for DNA extraction.

## 138 **Geochemical analysis**

139 The soil samples were dried at 55°C and crushed, before passing through a 2-mm  
140 sieve. The soil samples were mixed at a soil: water ratio of 1:5 (w/v), shaken well,  
141 and allowed to stand for 48 h. The supernatant was passed through a filter membrane

142 with a pore size of 0.45  $\mu\text{m}$  to prepare the test solution for the experiments. The soil  
143 electrical conductivity (EC) value was measured in a suspension with a soil:water  
144 ratio of 1:5 (w/v) using a CLEAN Conductivity Tester (CON30; FC Corporation,  
145 California, USA). The soil pH value was measured in a suspension with a soil:water  
146 ratio of 1:5 (w/v) using a pH meter (PB-10; Sartorius, Goettingen, Germany). The  
147 pore-water dissolved nitrate ( $\text{NO}_3^-$ ) and sulfate ( $\text{SO}_4^{2-}$ ) contents were analyzed by ion  
148 chromatography (DX-120, DIONEX, Bannockburn, IL, USA) [29]. The Total organic  
149 carbon (TOC) content (Calculated as carbon dioxide) was confirmed by using a  
150 high-frequency infrared Carbon-Sulfur Analyzer (LECO CS744, LECO Corporation,  
151 USA). Total nitrogen (TN) was analyzed using a Eurovector elemental analyzer  
152 (Isoprime-EuroEA 3000, Milan, Italy). The available nitrogen (AN) contents were  
153 determined with the alkaline digestion diffusion method. The total sulfur (TS) contents  
154 were measured using the infrared absorption method after high frequency combustion  
155 (High-speed Analyzer HWF-900A, Wuxi, China). Other trace metal(loid)s were analyzed  
156 by ICP-MS (ThermoFisher X-series, Franklin, MA, USA) and ICP-AES (TJA  
157 IRIS-Advantage, Franklin, MA, USA).

## 158 **DNA extraction, library construction, and metagenomic** 159 **sequencing**

160 The total DNA was extracted from each soil sample (0.5 g) using a PowerSoil DNA  
161 Extraction Kit (MoBio Laboratories, Carlsbad, CA, USA). The quantity and quality of

162 isolated DNA were evaluated using a NanoDrop spectrophotometer (ND-2000,  
163 Thermo Fisher Scientific, Waltham, MA, USA) and agarose gel electrophoresis  
164 (Bio-Rad, Hercules, CA, USA), respectively. The extracted DNA was stored at  $-20^{\circ}\text{C}$   
165 until further analysis, or at  $-80^{\circ}\text{C}$  for long-term storage.

166 DNA was fragmented to an average size of about 300 bp using Covaris M220  
167 (Gene Company Limited, China) for paired-end library construction. Paired-end  
168 library was prepared by using TruSeq<sup>TM</sup> DNA Sample Prep Kit (Illumina, San Diego,  
169 CA, USA). Adapters containing the full complement of sequencing primer  
170 hybridization sites were ligated to the Blunt-end fragments. Paired-end sequencing  
171 was performed on Illumina HiSeq3000 platform (Illumina Inc., San Diego, CA, USA)  
172 at Majorbio Bio-Pharm Technology Co., Ltd. (Shanghai, China) using HiSeq 3000 PE  
173 Cluster Kit and HiSeq 3000 SBS Kits according to the manufacturer's instructions  
174 ([www.illumina.com](http://www.illumina.com))

## 175 **Bioinformatics**

176 The 3' and 5' ends were stripped (<https://github.com/jstjohn/SeqPrep>) and low-quality  
177 reads were removed (<https://github.com/najoshi/sickle>). The software SOAPdenovo  
178 (<http://soap.genomics.org.cn>, Version 1.06) was employed to assemble short reads and  
179 K-mers were tested for each sample. The software Scaffolds was employed to gene  
180 prediction and annotation after with a length over 300 bp were extracted and broken  
181 into contigs without gaps. The software CD-HIT

182 (<http://www.bioinformatics.org/cd-hit/>) was employed to all sequences sequence  
183 identity (90% coverage) from gene sets with  $\geq 95\%$ , and were clustered as the  
184 non-redundant gene catalog using. After quality control, the software SOAPaligner  
185 (<http://soap.genomics.org.cn/>) was employed to mapped reads to representative genes  
186 with  $\geq 95\%$  identity, and the gene abundances were evaluated in each sample. The  
187 software BLASTP (Version 2.2.28+, <http://blast.ncbi.nlm.nih.gov/Blast.cgi>) was  
188 employed to taxonomic annotations by aligning non-redundant gene catalogs against  
189 NCBI NR database with cutoff:  $1e^{-5}$ (e-value). The software BLASTP (Version  
190 2.2.28+) was employed to annotation the KEGG pathway search against the Kyoto  
191 Encyclopedia of Genes and Genomes database (<http://www.genome.jp/keeg/>) with an  
192 cutoff:  $1e^{-5}$  (e-value).

## 193 **Statistical analyses**

194 Trimmomatic software was used to excise primers and for quality filtering with the  
195 original metagenomic sequences [30]. MetaPhlan2 software was then used to  
196 analyze the data and obtain the classifications for the microbial population with a  
197 degree of horizontal precision [31]. The species concentration in each sample type  
198 was calculated by comparing the mean and median relative abundances in the saline  
199 and nonsaline soil samples. R was used to conduct statistical analyses and to plot the  
200 taxonomic information at the genus level. The Shannon diversity index was calculated

201 using the “vegan” package [32]. The Bray–Curtis dissimilarity between different  
202 sample types was calculated using the R package “ecodist” [33].

203 KEGG Orthology (KO) functional profiling of the soil microbiota was performed  
204 using assemblies derived from whole-genome shotgun sequencing data. Low-quality  
205 reads were first trimmed from raw sequencing data using Trimmomatic. High-quality  
206 reads were assembled de novo into contigs using metaSPAdes [34] with the default  
207 parameters. Next, we performed gene prediction for these scaffolds using PROKKA  
208 V.1.11 [35] and the predicted proteins were assigned to the KO using the Kyoto  
209 Encyclopedia of Genes and Genomes (KEGG) Automatic Annotation Server.  
210 Trimmed high-quality reads located on the given scaffolds were counted to calculate  
211 the abundances of Kos in each sample using the Burrows–Wheeler Aligner [36]. The  
212 matrix was normalized by dividing the absolute amount of each functional gene by  
213 the total number of reads assigned to functional genes in each sample in order to  
214 determine the differential expression of microbial functional pathways in the saline  
215 and nonsaline soil samples.

216 The bacterial correlations in the saline and nonsaline soil samples were computed  
217 based on the relative abundance of each genus using SparCC with 100 bootstraps to  
218 estimate the  $p$ -values for co-occurrence network analysis. The correlation values  $p <$   
219 0.05 were retained. The co-occurrence network obtained for the microbial  
220 communities in the saline and nonsaline soil samples was visualized with Gephi

221 (version 0.9.1, <https://gephi.org/>). The closeness values and eigenvectors were  
222 calculated for the nodes to measure the node centralities in each network.

223 Community clustering was conducted based on the Bray–Curtis distance for  
224 principal coordinate analysis at the genus level, and ADONIS (“vegan”) analysis was  
225 performed to assess the similarities between groups and the significance of the  
226 differences between groups. Genera variation analysis to contrast the two soil sample  
227 types was conducted using the Wilcoxon rank sum test with R. Checks and  
228 corrections of the false discovery rate (FDR) were performed using the R program  
229 `fdrtool`.

## 230 **Results and Discussion**

### 231 **Soil characteristics of Tibetan Plateau**

232 In figure2, Soil geochemical analysis showed that the EC values determined for the  
233 saline soil were about  $9 \text{ ds} \cdot \text{m}^{-1}$ , and thus the soils were moderately saline [37]. The  
234 EC values of the nonsaline soil were less than  $4 \text{ ds} \cdot \text{m}^{-1}$ . The pH values were  $\sim 4.5$  for  
235 the saline soil and  $\sim 7.2$  for the nonsaline soil. TOC of saline and nonsaline soil were  
236 about 1.2% and about 4.1% respectively. The soil moisture contents were about 7%  
237 higher in nonsaline soil than the saline soil, possibly because salinization destroyed  
238 the physical structure of the soil. The nitrate, sulfate, and TS accumulations were  
239 significantly higher in the saline soil than the nonsaline soil, whereas TN and AN  
240 were significantly lower in the saline soil. Thus, the saline soil was acidic and the

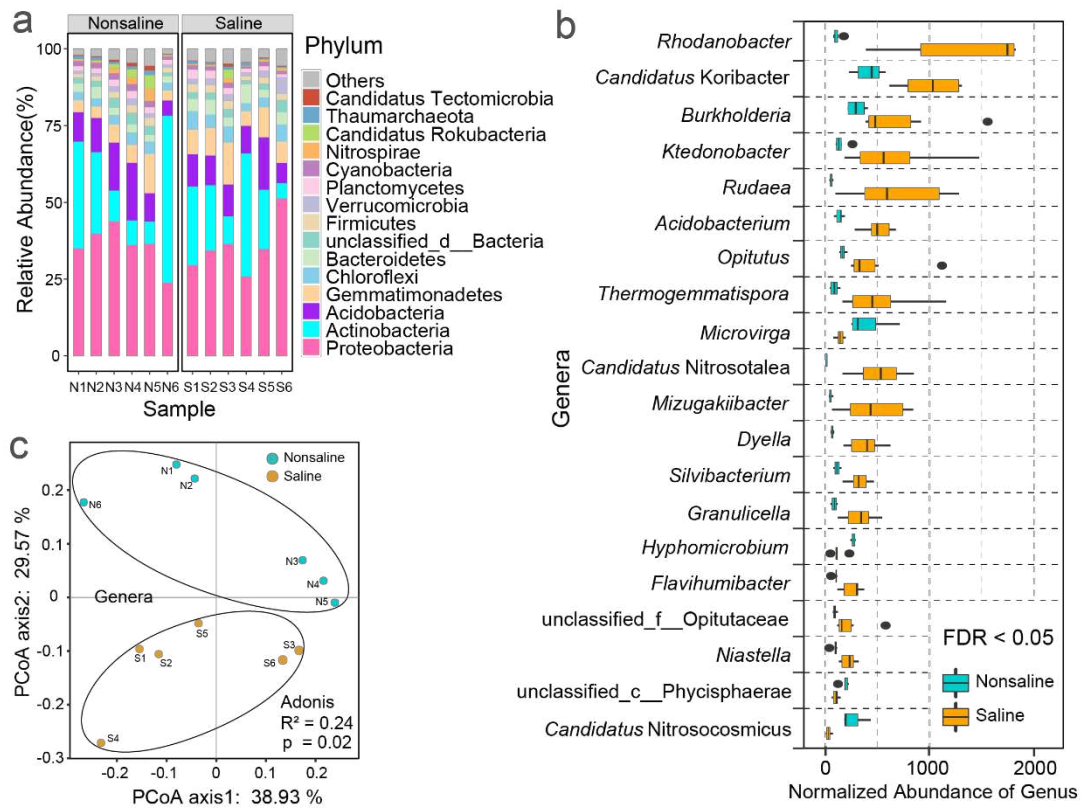
241 nutrient nitrogen contents were lower. The long-term accumulation of heavy  
242 metal(loid)s resulted in an extremely high Mn content. The levels of heavy  
243 metal(loid)s such as Zn, As, Cu, and Cr, and metal cations such as  $K^+$ ,  $Ca^{2+}$ , and  $Mg^{2+}$   
244 were also significantly higher in saline soil than nonsaline soil (Fig. S2). In general,  
245 the saline and nonsaline soil differed significantly in terms of most of the geochemical  
246 parameters (FDR < 0.05, Fig S2). The saline soil had a low pH, high salinity, and low  
247 nutrient levels, and it was also affected by the extreme unique climate of the Tibetan  
248 Plateau, including cold, hypoxia, and strong ultraviolet radiation. Microorganisms  
249 may produce a series of community changes and genetic selection under such  
250 environmental conditions.

## 251 **Bacterial community in saline and nonsaline soil of Tibetan** 252 **Plateau**

253 After removing low-quality reads of metagenomic sequencing, the quality control  
254 results (Table S1) and predicted open reading frames after assembly (Table S2)  
255 showed that the average Shannon index was 5.43 for saline soil and that for nonsaline  
256 soil was 5.35 (Table S3). In all samples, bacteria accounted for approximately 98.07%  
257 of the total sequences, archaea accounted for approximately 1.32%, and fungi  
258 accounted for only 0.01%. The microbial community was dominated by bacteria, and  
259 the proportions of archaea and fungi were extremely low. At the microbial phylum

260 level, the sequences were dominated by Proteobacteria, Actinobacteria, Acidobacteria,  
 261 Gemmatimonadetes, Chloroflexi, and other phyla (Fig. 1a).

262



263

264 **Figure 1. Composition and differences in saline and nonsaline soil on the Tibetan**

265 **Plateau.** a. Bacterial composition at the phylum level in saline and nonsaline soil

266 samples of Tibetan Plateau. b. Top 20 genera with significant differences (FDR <

267 0.05) in saline (orange) and nonsaline (cyan) soil samples of Tibetan Plateau, the total

268 number of reads is normalized to 100000. c. Principal coordinate analysis of saline

269 (orange) and nonsaline (cyan) soil samples based on the composition and abundances

270 of the bacterial communities at the genus level.

271

272 By analyzing the differences in the bacterial compositions in two types of soil  
273 samples (Wilcoxon's test, FDR < 0.05, Fig. 1b), we found that the significantly  
274 enriched bacteria in the saline soil had different metabolic strategies. Most were  
275 heterotrophic bacteria, but some were chemoautotrophs, such as *Rhodanobacter*,  
276 *Granulicella*, and *Acidobacterium*. The dominant significantly enriched bacterial  
277 groups associated in the carbon and nitrogen cycles identified in nonsaline soil. For  
278 example, *Microvirga* and *Hyphomicrobium* have denitrification functions [38, 39],  
279 and *Candidatus Nitrosocosmicus* has ammonia oxidation and carbon fixation  
280 capacities [40]. The bacteria in saline soil were found to have specific environmental  
281 adaptations (such as chemoautotrophs and obligate acidophilic), whereas the  
282 dominant bacteria in nonsaline soil have greater capacity for carbon and nitrogen  
283 assimilation. PCoA showed that all of the saline soil samples clustered together and  
284 those in nonsaline soil samples formed another cluster, thereby indicating that soil  
285 salinization led to significant differences in the bacterial community structure (Fig.  
286 1c).

287 The results of the functional abundance based on the KEGG database (Fig. S3a)  
288 showed that significant differences in functional genes related to environmental stress  
289 resistance (ultraviolet radiation resistance, temperature change response, oxygen  
290 limitation response, and salinity adaptation) and important biogeochemical processes  
291 (e.g., carbon fixation, nitrogen metabolism, sulfur metabolism, methane metabolism,  
292 and heavy metal resistance). PCoA based on the functional composition showed (Fig.

293 S3b and c) that two separate clusters were formed at both module and KO levels,  
294 indicating that salinization also led to significant differences in the soil bacterial  
295 functions (ADONIS,  $p$ -value < 0.05). However, the certain bacterial metabolism  
296 related to different element cycles and environmental stress responses should be  
297 revealed deeply.

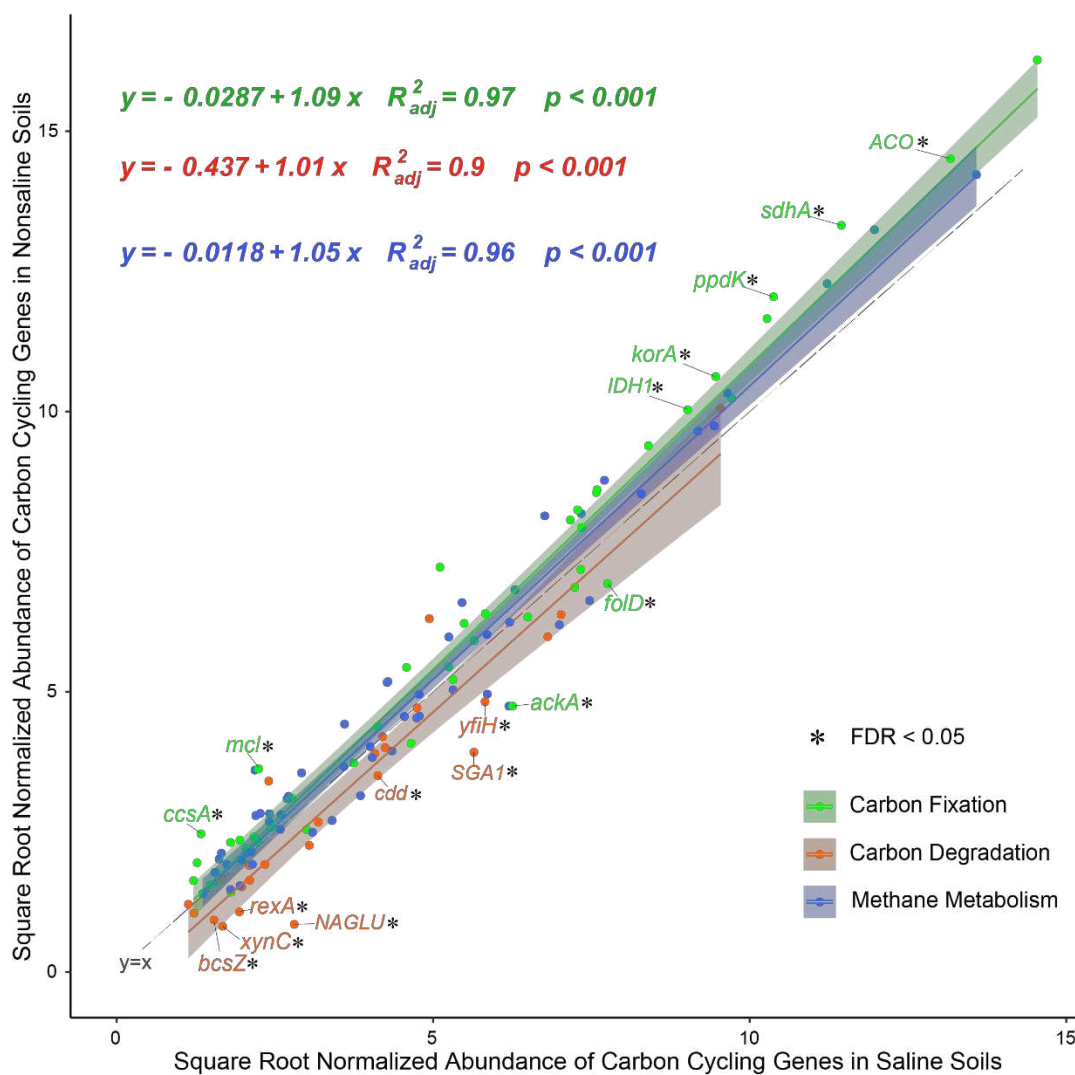
## 298 **Metabolic pathways in saline and nonsaline soil samples of** 299 **Tibetan Plateau**

### 300 **Carbon cycling**

301 The carbon cycle mainly comprises carbon fixation, carbon degradation, and methane  
302 metabolism, which is important for microorganisms in the soil to obtain energy and  
303 materials[41]. The carbon fixation pathways (Fig. S4a) in all the samples were mainly  
304 composed of the reductive citrate (rTCA) cycle, hydroxypropionate hydroxybutylate  
305 (3-HP/4-HB) cycle, crassulacean acid metabolism (CAM) pathway, and Wood–  
306 Ljungdahl (WL) pathway. In Fig. 2, only the abundances of the *ackA* and *fold* genes  
307 were significantly higher in saline soil than nonsaline soil, and these genes are  
308 involved in the 3-HP/4-HB cycle and WL pathway, respectively. Thus, the genes such  
309 as *korA*, *sdhA* and *ppdK* with significantly higher abundances in saline soil  
310 participated in the 3-HP/4-HB cycle and WL pathway, whereas the genes with  
311 significantly higher abundances in nonsaline soil mainly participated in the rTCA  
312 cycle. The rTCA cycle is prevalent in anaerobic bacteria that are adapted to hypoxic

313 environments on the Tibetan Plateau and this cycle only requires two ATP equivalents  
 314 to form pyruvate [42]. The abundance of the WL pathway was probably higher  
 315 because of its extremely low energy consumption (requirement < 1 ATP) and  
 316 requirement for strict anoxic conditions [43]. Thus, low nutritional availability and  
 317 extreme environments explain why the rTCA cycle and WL pathway predominate in  
 318 the soil on the Tibetan Plateau, where the 3-HP/4-HB cycle pathway are adaptations  
 319 to the nutritional deficiencies, respectively.

320



321

322 **Figure 2. The ratio of genes in carbon cycling pathway in saline and nonsaline**  
323 **soil on the Tibetan Plateau.** The black dotted line equation “ $y = x$ ” indicates that the  
324 horizontal and vertical axes are equal. Green, red, and blue represent genes of carbon  
325 fixation, carbon degradation, and methane metabolism pathways, respectively. Genes  
326 with significant differences ( $FDR < 0.05$ ) are marked in the corresponding colors and  
327 connected with short lines. The total number of reads is normalized to 100000.

328

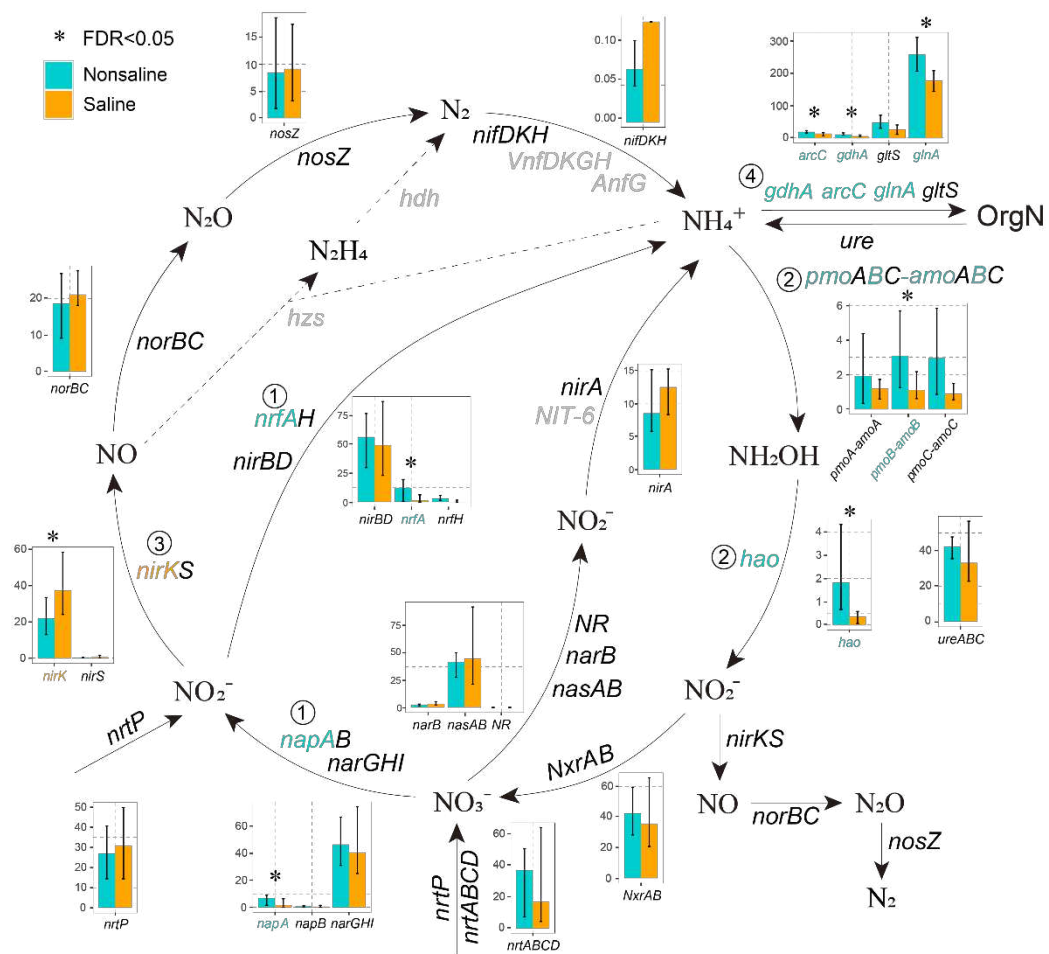
329 In the carbon degradation pathway (Fig. 2), the genes with significantly higher  
330 abundances in saline soil included genes related to starch degradation comprising *cdd*  
331 and *SGAI*, chitin degradation gene *NAGLU*, lignin degradation gene *yfiH*, cellulose  
332 degradation gene *bcsZ*, hemicellulose degradation gene *xynC*, and *rexA*, indicating  
333 that the potential for carbon degradation was greater in the saline soil. Interestingly,  
334 the abundances of genes associated with the degradation of labile carbon (starch,  
335 pectin, and hemicellulose) and recalcitrant carbon (cellulose, chitin, and lignin) were  
336 higher in the saline soil, possibly because these mechanisms allow microorganisms to  
337 maintain their ecosystem functions in the short term in saline soil. In addition, these  
338 mechanisms may also explain why the TOC contents were significantly lower in  
339 saline soil than nonsaline soil, and the collapse of farmland ecosystems may occur if  
340 saline soil remains oligotrophic for a long time [24, 25]. There were no significant  
341 differences in the abundances of genes related to methane metabolism in the two soil  
342 types (Fig. 2 and Fig. S4b). The lack of significant differences in abundances of genes

343 related to this process indicates that salinization of the soil had no significant impacts  
344 on methane metabolism.

### 345 **Nitrogen cycling**

346 The nitrogen cycle is one of the crucial soil nutrient cycle processes for the growth of  
347 crops and it is driven by soil microorganisms with specific functions [44]. The  
348 abundances of genes related to dissimilatory nitrate reduction and denitrification in  
349 the soil microbial nitrogen cycle differed significantly in saline and nonsaline soil (Fig.  
350 3), but they did not differ significantly in the nitrate assimilation reduction pathway.

351



352

353 **Figure 3. Differences in the abundance of genes related to nitrogen cycling in the**

354 **saline (orange) and nonsaline (cyan) soil on the Tibetan Plateau.** Bar plots show

355 the normalized abundances of nitrogen cycling genes. Significantly different (FDR <

356 0.05) genes are marked with “\*” and circled numbers. Undetected genes are indicated

357 in gray. Circled numbers identify genes with significant differences: 1, dissimilatory

358 nitrate reduction; 2, nitrification; 3, denitrification; and 4, organic nitrogen conversion.

359 The total number of reads is normalized to 100000.

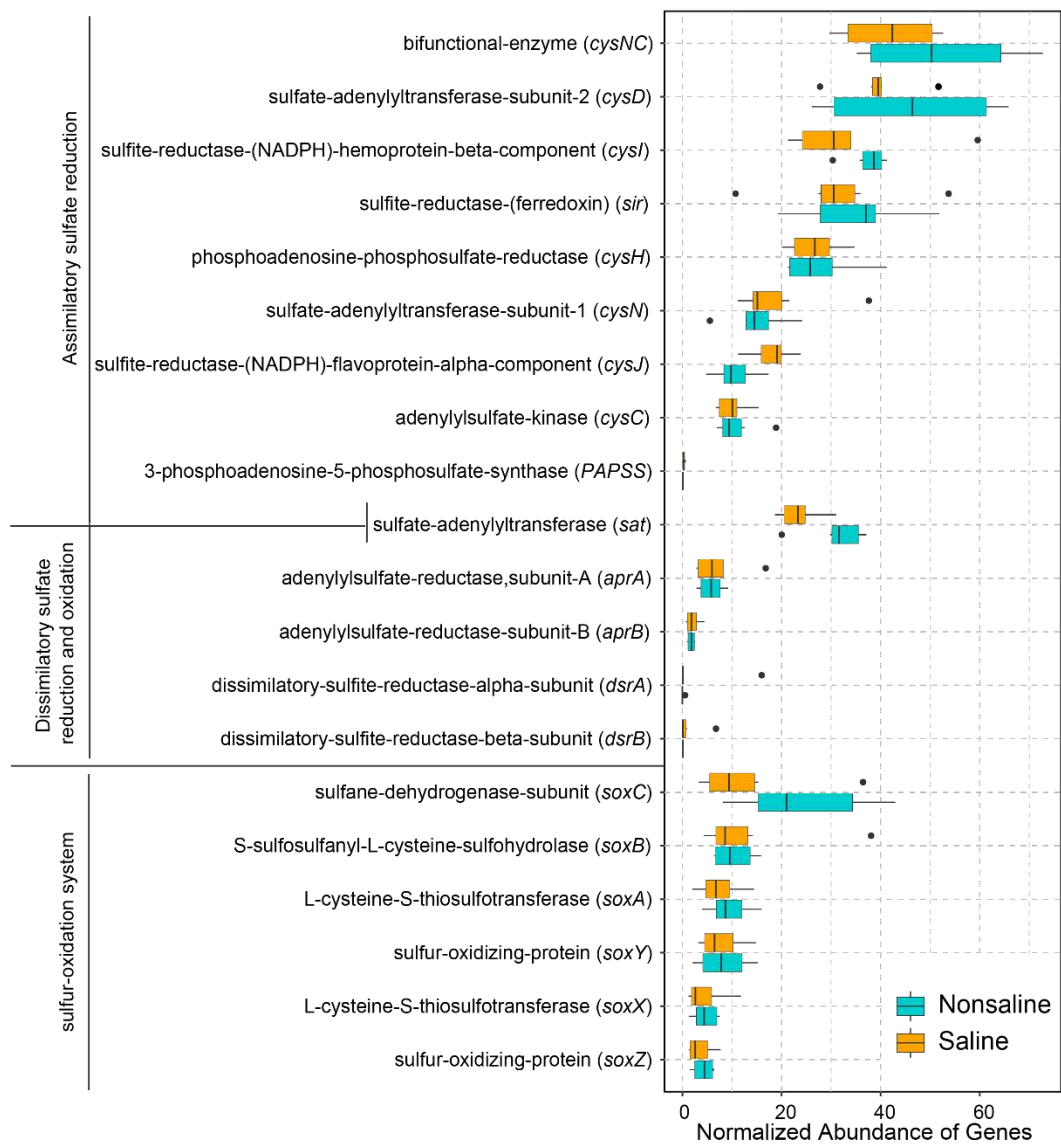
360

361 In the denitrification pathway, the abundance of gene *nirK* (nitrite reductase  
362 catalyzing N<sub>2</sub>O to NO) was significantly higher in saline soil (FDR < 0.05) than  
363 nonsaline soil. The presence of higher amounts of NO is likely to proceed forward to  
364 produce more N<sub>2</sub>O. In saline soil, bacteria have the potential to produce more NO and  
365 N<sub>2</sub>O via denitrification, and the abundances of genes *nosZ* that could reduce N<sub>2</sub>O  
366 were lower in saline soil than nonsaline soil, which were resulted in more NO and  
367 N<sub>2</sub>O produced in saline soil. The abundances of the dissimilatory nitrate reduction  
368 genes *napA* and *nrfA* were significantly higher (FDR < 0.05) in saline soil than  
369 nonsaline soil (Fig. 3), demonstrating that the potential for ammonia conversion was  
370 higher in nonsaline soil. Significantly higher abundances were found in nonsaline soil  
371 of the gene *gdhA* encoding the enzyme that catalyzes the conversion of ammonia to  
372 L-glutamate, which are all involved in the conversion of ammonia to glutamic acid  
373 (FDR < 0.05). It is indicated that more ammonia could be converted into organic  
374 nitrogen and this is beneficial for the production of crops. Microorganisms need to  
375 synthesize large amounts of amino acids to resist environmental pressure [45].  
376 Therefore, the input of ammonia is critical for the microbial community.

## 377 **Sulfur metabolism**

378 Due to the high input of sulfate in saline soil, we analyzed the differences in the genes  
379 abundance of three pathways related to sulfur metabolism (assimilatory sulfate  
380 reduction, dissimilatory sulfate reduction and oxidation, and SOX system) (Fig. 4).

381 The abundances of genes related to environmental sulfide absorption were  
 382 significantly lower in saline soil, but the abundances of genes associated with the  
 383 elimination of toxic intracellular sulfide were significantly higher.  
 384



385  
 386 **Figure. 4. Difference in abundances of sulfur cycling genes in saline (orange) and**  
 387 **nonsaline (cyan) soil on the Tibetan Plateau.** The total number of reads is  
 388 normalized to 100000.  
 389

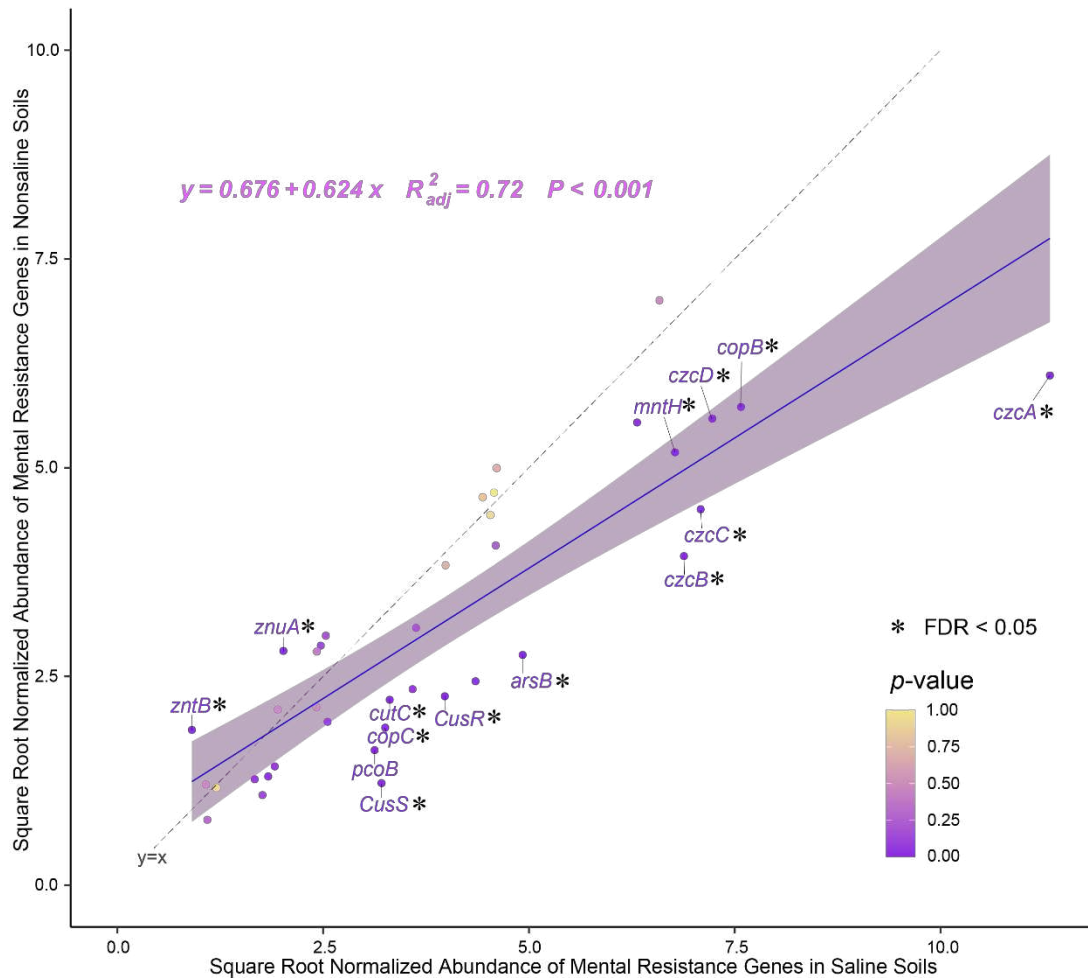
390 First, in saline and nonsaline soil, the abundance was high for the assimilatory  
391 sulfate reduction module that consumes sulfate in the environment and ultimately  
392 synthesizes sulfur-containing amino acids. This pathway was probably dominant  
393 because of the extremely high sulfate content in saline soil and the large demand for  
394 amino acids in the bacterial community. Second, in both soil types, the abundance  
395 was low for the dissimilatory sulfate reduction and oxidation module that produces  
396 energy and inorganic sulfides, and the abundance of *dsrAB* (dissimilatory sulfite  
397 reductase) was extremely low, probably because “reverse” sulfite reductase (*dsr*) is  
398 not necessary for the oxidation of sulfide or thiosulfate, and *sat* (encoding the enzyme  
399 that catalyzes the conversion of sulfate to Adenylyl sulfate) and *aprAB*  
400 (adenylylsulfate reductase) participate in the energy production process but they  
401 produce cytotoxic sulfites, so their abundances were also low. Finally, the abundance  
402 of the *soeBC* gene encoding the enzyme in the SOX system that catalyzes the  
403 conversion of sulfite into sulfate was significantly higher in saline soil, and this  
404 enzyme is important for sulfite oxidation in the cytoplasm (Fig. S5). The oxidation of  
405 sulfur can reduce the toxicity of sulfite in cells [46], as well as providing electrons and  
406 energy to cells [47].

## 407 **Metal resistance**

408 In this study, the abundances of heavy metal(loid) resistance genes such as *copB*, *cutC*,  
409 *cusRS*, and *pcoB* genes that confer tolerance to copper and the manganese transport

410 gene *mntH* were significantly higher in saline soil (Fig. 5). The differences in the  
411 functional genes related to heavy metal absorption showed that the gene *arsB* related  
412 to arsenic absorption had a significantly higher abundance in saline soil (Fig. 5). Both  
413 soil types had high abundances of the arsenate reductase gene (*arsC*), but the  
414 abundance of the arsenite oxidase gene (*aoxAB*) was extremely low because the  
415 hypoxic environment promoted the migration of arsenic [48]. The accumulation of  
416 arsenite in saline soil on the Tibetan Plateau has toxic effects on microorganisms and  
417 crops. However, the abundance of gene *arsH* (arsenical resistance protein) was  
418 extremely low in both soil types (Fig. S6), and thus, the soil bacteria did not have a  
419 high capacity to resist the accumulation of arsenic in study area.

420



421

422 **Figure 5. Abundance of heavy metal(loid) resistance genes in saline and**

423 **nonsaline soil on the Tibetan Plateau.** The black dotted line with the equation “y =

424 x” indicates that the horizontal and vertical axes are equal. Genes with significantly

425 different abundances (FDR < 0.05) are marked in purple and connected with short

426 lines. The total number of reads is normalized to 100000.

427

428 These results indicate that two main mechanisms mediate microbial resistance to

429 the toxicity of heavy metal(loid)s in saline soils on the Tibetan Plateau, i.e., the efflux

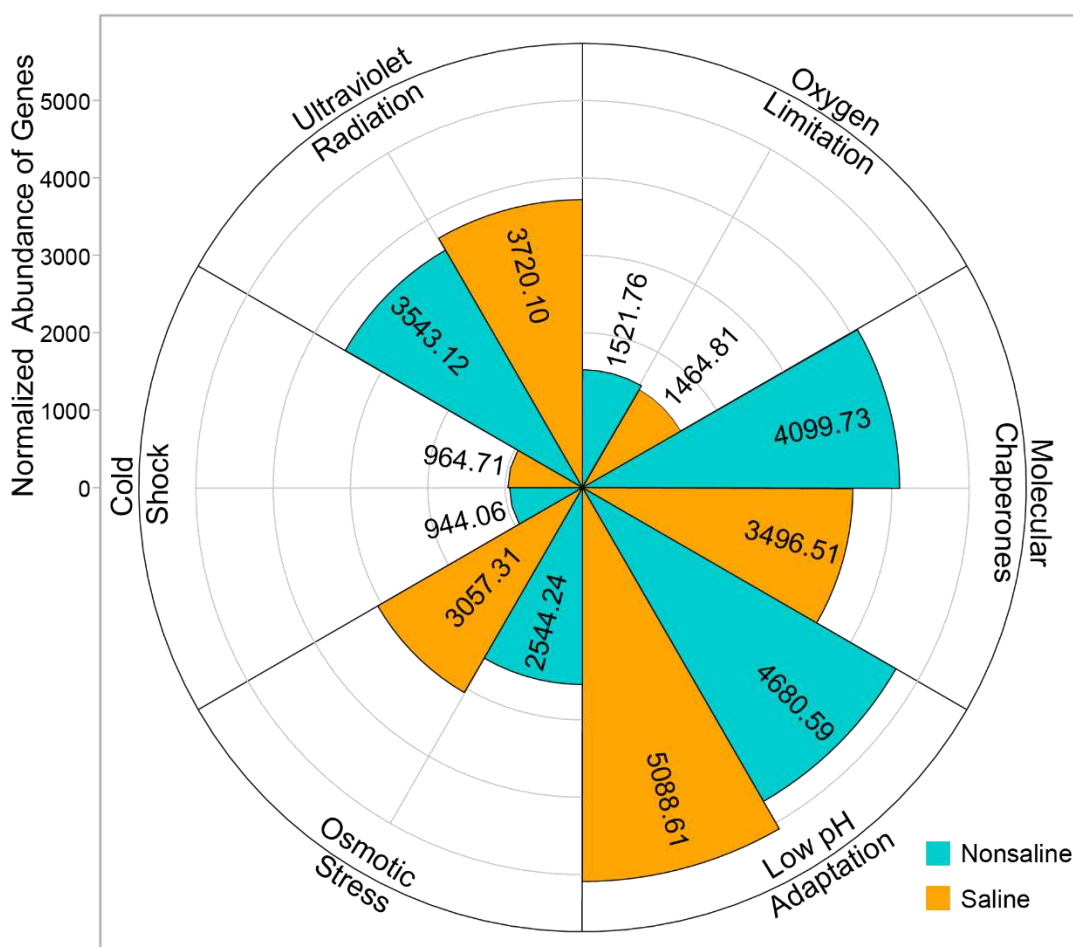
430 of excessive concentrations of heavy metal(loid) ions from cells and expressing

431 proteins that confer tolerance of heavy metal(loid) ions. However, bacteria to resist

432 increasing concentrations of heavy metal(loid)s is possibly not sufficient for  
 433 increasing concentration of heavy metal(loid) ions in the soil of Tibetan Plateau,  
 434 which should be studied in future research.

### 435 Environmental stress response

436



437

438 **Figure 6. Abundance of the environmental stress resistance genes.** The total

439 number of reads is normalized to 100000.

440

441 Ultraviolet radiation resistance, the nucleotide excision repair pathway, and  
 442 photoreactivation (DNA repair via the photolysis enzyme encoded by the *phrB* gene)

443 are applied by bacteria to avoid and repair damage due to ultraviolet radiation [49]  
444 (Fig. 6). The abundances of the *recNO* and *alkB* genes associated with DNA repair  
445 were significantly higher in saline soil due to more DNA damage in saline soil (Fig.  
446 S8). Bacteria adapt to cold environments mainly through cold shock genes *cspA*, *desK*,  
447 and *desR*, which encode enzymes that protect cells from ice crystal damage, and that  
448 maintain the transcription and translation processes within cells [50, 51], and via lipid  
449 desaturases (*desA1*, *desA2*, and *desC*; Fig. S7) and the synergy among unsaturated  
450 fatty acid synthesis genes *fabAB* (anaerobic) and *desAB* (aerobic), which are  
451 responsible for synthesizing short-chain unsaturated fatty acids embedded in the cell  
452 membrane to maintain the cell membrane fluidity and avoid film hardening at low  
453 temperatures [52, 53]. These genes were abundant in the two soil types and the  
454 abundance of *fabAB* was higher than that of *desAB* due to low oxygen levels on  
455 Tibetan Plateau (Fig. S7). Bacteria express large amounts of catalase and peroxidase  
456 when responding to oxygen limitation stress [40]. Thus, the abundances of the *cydB*,  
457 *fnr*, and *oxyR* genes were significantly higher in saline soil (Fig. S7), whereas the *katE*  
458 (catalase) gene was more abundant in nonsaline soil, and the enzyme encoded by *katE*  
459 also acts as a cross-protection protein to help cells cope with environmental pressures.  
460 The response mechanisms to oxygen limitation differed between the two soil types.  
461 Molecular chaperones help protein folding and refolding to enhance stress resistance  
462 [54], and many of these genes had high abundances in the two sample types (Fig. S7).  
463 However, the abundances of *dank* and *groEL* were significantly (FDR < 0.05) higher

464 in CK, whereas *grpE* and *pccA* were more abundant in SA, and the abundances of  
465 major molecular chaperone genes were higher in nonsaline soil than saline soil (Fig.  
466 S7), which lacked sufficient energy and substrates to synthesize the required molecular  
467 chaperones.

468 In response to high salinity and low pH, the abundance of the K<sup>+</sup> high-affinity  
469 transport system (*kdpABC*) was significantly higher in saline soil (Fig. S7). Bacteria  
470 generate an inward positive membrane potential through the active inflow of K<sup>+</sup> to  
471 partially deflect the inward flow of protons [55], as well as helping cells to resist the  
472 stress due to high osmotic pressure. The metabolism of proton buffer molecules can  
473 also maintain the pH in the cytoplasm, and the abundance of the phosphate uptake  
474 gene *pstS* was significantly higher in saline soil (Fig. S7). Cross-protective genes  
475 encoding proteins (*osmC*, *dps*, and *katE*) that maintain the normal life activities of  
476 cells under high osmotic pressure were abundant in saline soil, where the abundance  
477 of *osmC* was significantly higher. In addition, the microbial self-synthesizing glycine  
478 betaine gene *gbsAB* was more abundant in nonsaline soil, whereas proline and glycine  
479 betaine absorption genes (*opuABCD*, *proP*, *putABP*, etc.) were more abundant in  
480 saline soil (Fig. S7), probably because the energy consumed by the synthetic permeate  
481 was higher than that absorbed from the environment. Therefore, the soil bacteria in  
482 saline soil were deficient in substances and energy, so they employed low energy  
483 consumption mechanisms to absorb K<sup>+</sup>, phosphate, and osmotic substances from the

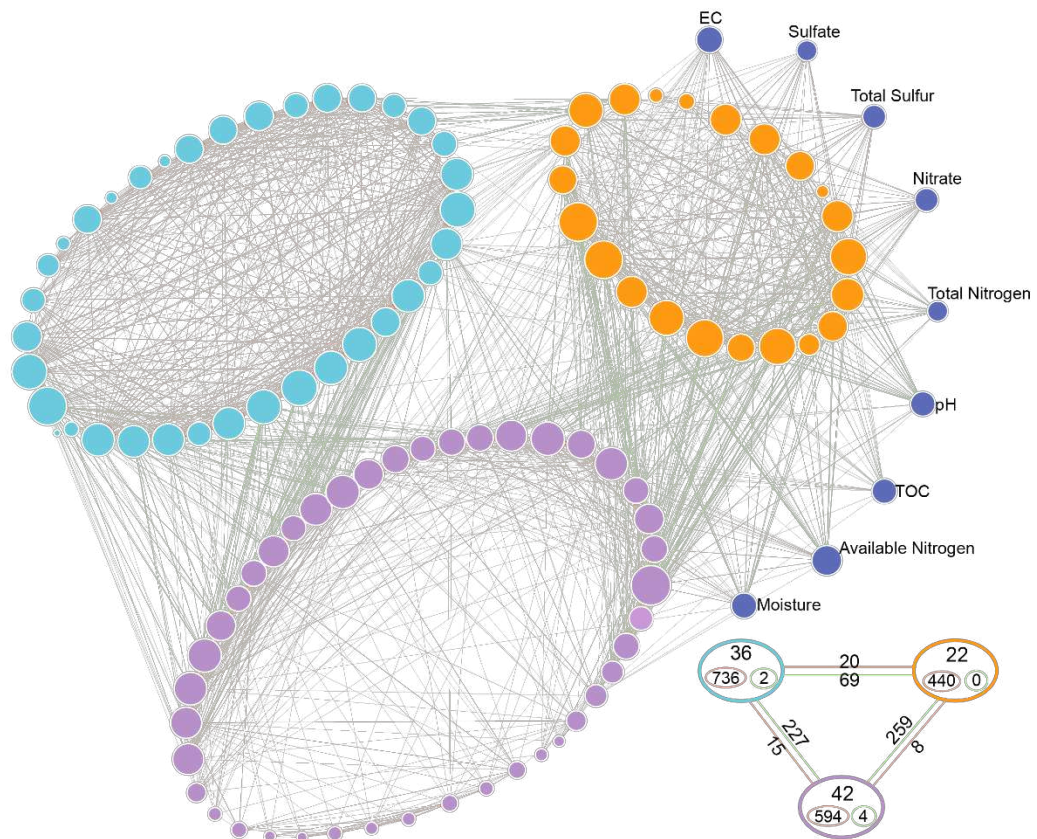
484 environment, as well as synthesizing a small amount of protective proteins to resist  
485 the low pH and high osmotic pressure stresses.

486 Thus, the bacterial community in saline soil was affected by more extreme  
487 environmental stresses than that in nonsaline soil. Low pH and high osmotic pressure  
488 resistance genes were more abundant, and the abundances of molecular chaperone  
489 genes were significantly lower. Genes related to adaptability to the specific climatic  
490 conditions on the Tibetan Plateau were abundant and the differences in their  
491 abundances in the two soil types were not obvious.

## 492 **Effects of physicochemical parameters on microbial** 493 **community and metabolic capacity**

494 Co-occurrence network analysis based on the bacterial genera, functional genes, and  
495 environmental factors was constructed in order to understand how environmental  
496 factors affect the complex bacterial community structure and functions in saline and  
497 nonsaline soils on the Tibetan Plateau (Figs. 7 and S8). The network based on the  
498 bacterial community and environmental factors contained three bacterial modules  
499 (Table S3). The main negative correlations were found between these three modules,  
500 but the bacterial genera within the same module were mainly positively correlated  
501 (Fig. 7).

502



503

504 **Figure 7. Network of the top 100 dominant genera and physicochemical**

505 **parameters.** A connection denotes a Spearman's correlation coefficient with a

506 magnitude greater than 0.6 (positive correlation = red lines) or less than -0.6

507 (negative correlation = green lines) and statistically significant ( $p$ -value < 0.05). The

508 size of each node is proportional to the number of connections (i.e., degree). The

509 thickness of each connection between two nodes (i.e., edge) is proportional to the

510 Spearman's correlation coefficient (i.e., weight), ranging from  $|0.6|$  to  $|1|$ . The network

511 is colored according to the modules, where the nodes clustered in the same module

512 share the same color. The lower right corner is a schematic diagram, and the large

513 circles represent three modules based on network analysis, and the positions are

514 corresponding. In the large circles, the top number indicates the number of nodes, the  
515 red circle and the number indicate positive correlation within the module, and the  
516 green indicates negative correlation. Between the large circles, red lines and numbers  
517 indicate positive correlations, and green lines and numbers indicate negative  
518 correlations.

519

520 Module 0 (Orange) contained a total of 22 nodes and most nodes (> 50%)  
521 represented microbial genera with a significant (FDR < 0.05) higher abundance in  
522 saline soil. Most of the genera are chemoautotrophic and acidophilic bacteria (Table  
523 S5 and Fig. 1a), which have strongest correlations with the soil physicochemical  
524 parameters, including positive correlations with EC, sulfate, total sulfur, and nitrate,  
525 but mostly negative correlations with pH, TN, AN moisture, and TOC (Fig. 7).  
526 Module 1 (purple) contained 42 nodes. All of the genera are high abundant in the two  
527 soil types. These genera had strong positive correlations with the soil moisture, TOC,  
528 and AN, weak positive correlations with TN and pH, and mostly negative correlations  
529 with other environmental factors (Fig. 7). Module 2 (cyan) contained 36 nodes, and  
530 these genera were in saline and nonsaline soil. They had very weak negative  
531 correlations with TN and pH, and almost no correlations with other environmental  
532 factors. Overall, EC, AN, moisture, TOC, and pH were the most influential  
533 environmental factors. Bacterial community responded to the environmental factors  
534 by forming different functional groups (Fig. 7), indicating that the stress due to

535 salinity indeed altered the topological roles of microbes and reorganized the keystone  
536 populations [56].

537 The network constructed based on the functional genes and environmental factors  
538 in different metabolic pathways (Fig. S8 and Table S4) showed that the main physical  
539 and chemical parameters in saline soil (EC, pH, TOC, moisture, AN, TS, etc.)  
540 affected the key biogeochemical cycles for C, N, S, As, and other elements in the soil  
541 (Fig. S8). TOC was significantly positively correlated with rTCA cycling which was a  
542 high energy efficiency conversion rate pathway in the carbon cycle. However, TOC  
543 was significantly negatively correlated with the WL pathway, which may have been  
544 related to the extremely low energy consumption and strict anaerobic requirements of  
545 this pathway. In addition, TOC, moisture, and pH were significantly negatively  
546 correlated with the main carbon degradation genes (*cdd*, *SGAI*, *rexA*, *xynC*, *bcsZ*, and  
547 *NAGLU*), and the high abundance of carbon degradation genes resulted in a  
548 significant decrease in the soil TOC concentration (Fig. 3). EC was negatively  
549 correlated with carbon fixation genes and positively correlated with carbon  
550 degradation genes, indicating that high salinity led to the rapid degradation of organic  
551 carbon for the bacterial requirements for substrates and energy. Most of the genes in  
552 nitrogen cycle were also positively correlated with TN, AN moisture, and pH, but  
553 negatively correlated with EC (Fig. S8). In particular, the abundance of gene *nirK* was  
554 significantly negatively correlated with TN, but significantly positively correlated  
555 with pH, indicating that the denitrification process in saline soil was affected by

556 changes in the soil physicochemical properties, and the long-term accumulation of  
557 salinity may have led to the accumulation of nitrate and enhanced denitrification. In  
558 addition, sulfate and total sulfur were significantly negatively correlated with the  
559 sulfate absorption gene *cysAPUW*, but significantly positively correlated with the  
560 sulfur oxidation gene *soeABC*, while the key gene *sat* in the sulfate reduction pathway  
561 was significantly negatively correlated with EC. These results suggest that the  
562 accumulation of sulfide in saline have resulted in the bacteria producing more sulfur  
563 oxidation genes to synthesize more sulfate. The secondary accumulation of salt would  
564 happen in the soil. Moreover, the soil moisture and pH were negatively correlated  
565 with arsenic resistance genes, whereas EC had positive correlations. Overall, high  
566 salinity and the accompanying changes in the soil properties had significant impacts  
567 on the microbial community and its metabolic network, with significant increases in  
568 the chemoautotrophic and acidophilic bacterial modules, as well as effects on other  
569 heterotrophic bacteria modules related to the carbon and nitrogen cycles. The bacterial  
570 community in the saline soil is likely to consume more soil organic carbon to increase  
571 denitrification and intensify the oxidation of sulfur.

## 572 **Conclusions**

573 Global warming has caused the melting of glaciers and the repeated freezing and  
574 thawing of the permanently frozen soil on the Tibetan Plateau, resulting in a sudden  
575 increase in the water volume and the exposure of rock formations, where the water

576 flow has washed over these mineral-rich rock formations into rivers to subsequently  
577 increase the soil salinity via irrigation. In this study, we found that the salinization of  
578 the soil was accompanied by increased acidity and the accumulation of metal. People  
579 who live along the rivers on the Tibetan Plateau are affected by the risk of  
580 increasingly saline farming soil. Soil salinization significantly changed the bacterial  
581 communities on the Tibetan Plateau, and chemoautotrophic and acidophilic bacteria  
582 became dominant. In addition, the key biogeochemical cycle function clusters  
583 changed. Carbon degradation, denitrification, and sulfur oxidation gene clusters were  
584 highly abundant in saline soils, which were associated with the loss of soil organic  
585 matter, increased emissions of NO and N<sub>2</sub>O, and higher sulfate levels in local area.  
586 The bacterial community adapting to saline soil did not alleviate the degree of soil  
587 salinity, and bacterial community is likely to consume more energy to cope with the  
588 extreme climate under saline soil conditions due to the unique features of the Tibetan  
589 Plateau. The Yalong River Basin in the study area is a major tributary in the middle  
590 reaches of the Yarlung Zangbo River and the most important agricultural area in  
591 Shannan City, Tibet. The continuous salinization of agricultural soil along this river  
592 will have severe detrimental effects on the local economy and environment. Soil  
593 salinization also becomes one of the most direct forms of feedback on the Tibetan  
594 Plateau in response to global climate change.

## 595 **Declarations**

### 596 **Ethics approval and consent to participate**

597 Not applicable.

### 598 **Consent for publication**

599 Not applicable.

### 600 **Availability of data and materials**

601 The raw sequence data reported in this paper have been deposited in the Genome  
602 Sequence Archive (Genomics, Proteomics & Bioinformatics 2017) in National  
603 Genomics Data Center (Nucleic Acids Res 2021), China National Center for  
604 Bioinformation / Beijing Institute of Genomics, Chinese Academy of Sciences, under  
605 accession number CRA003771 that are publicly accessible at  
606 (<http://bigd.big.ac.cn/gsa/s/6AYB1I5n>).

### 607 **Competing interests**

608 The authors declare that they have no competing interests.

### 609 **Funding**

610 This research was supported by the Science and Technology Program of Tibet  
611 Autonomous Region (XZ201901NB06 granted to XY Guan), The Fundamental

612 Research Funds for the Central Universities (2652019077, grant to XY Guan) and  
613 National Natural Science Foundation of China (41731282 granted to XY Guan). The  
614 authors would like to thank Cidan ZX, Yuxuan X, Minghan W and Yanming Z for  
615 their assistance with this study.

## 616 **Authors' contributions**

617 YL, XG and LH were responsible for collection of samples. XW performed DNA  
618 extractions and preparation. LH, CQ and XL measured and analyzed the  
619 environmental factors. YL and YC performed sequence assembly, annotation,  
620 analysis. QL and YL visualized most of figures. XL and XG developed the project  
621 design and provided project oversight. Both YL, XW and XG contributed to the  
622 writing of the manuscript. All authors read and approved the final manuscript.

## 623 **Acknowledgements**

624 The authors thank Xianzhuang Li and Jiayang Zhao of Beijing Key Laboratory of  
625 Water Resources and Environmental Engineering, China University of Geosciences  
626 (Beijing), Beijing, China, for their assistance in soil sample processing and physical  
627 and chemical testing.

628

629

630

## References

- 632 1. Kang S, Xu Y, You Q, Flügel W-A, Pepin N, Yao T: **Review of climate**  
633 **and cryospheric change in the Tibetan Plateau.** *Environmental*  
634 *Research Letters* 2010, **5**(1).
- 635 2. Guan X, Wang J, Zhao H, Wang J, Luo X, Liu F, Zhao F: **Soil bacterial**  
636 **communities shaped by geochemical factors and land use in a**  
637 **less-explored area, Tibetan Plateau.** *BMC genomics* 2013, **14**(1):820.
- 638 3. Qiu J: **China: the third pole.** *Nature* 2008, **454**(7203):393-396.
- 639 4. Zhang H, Fan J, Wang J, Cao W, Harris W: **Spatial and temporal**  
640 **variability of grassland yield and its response to climate change**  
641 **and anthropogenic activities on the Tibetan Plateau from 1988 to**  
642 **2013.** *Ecological Indicators* 2018, **95**:141-151.
- 643 5. Rillig MC, Ryo M, Lehmann A, Aguilar-Trigueros CA, Buchert S, Wulf  
644 A, Iwasaki A, Roy J, Yang G: **The role of multiple global change**  
645 **factors in driving soil functions and microbial biodiversity.**  
646 *Science* 2019, **366**(6467):886-890.
- 647 6. Cheng G, Wu T: **Responses of permafrost to climate change and their**  
648 **environmental significance, Qinghai - Tibet Plateau.** *Journal of*  
649 *Geophysical Research: Earth Surface* 2007, **112**(F2).
- 650 7. Luo S, Wang S, Tian L, Shi S, Xu S, Yang F, Li X, Wang Z, Tian C:  
651 **Aggregate-related changes in soil microbial communities under**  
652 **different ameliorant applications in saline-sodic soils.** *Geoderma*  
653 2018, **329**:108-117.
- 654 8. Che R, Wang Y, Li K, Xu Z, Hu J, Wang F, Rui Y, Li L, Pang Z, Cui  
655 X: **Degraded patch formation significantly changed microbial**  
656 **community composition in alpine meadow soils.** *Soil and Tillage*  
657 *Research* 2019, **195**:104426.
- 658 9. Li HY, Webster R, Shi Z: **Mapping soil salinity in the Yangtze delta:**  
659 **REML and universal kriging (E-BLUP) revisited.** *Geoderma* 2015,  
660 **237-238**:71-77.
- 661 10. Zovko M, Romić D, Colombo C, Di Iorio E, Romić M, Buttafuoco G,  
662 Castrignanò A: **A geostatistical Vis-NIR spectroscopy index to**  
663 **assess the incipient soil salinization in the Neretva River valley,**  
664 **Croatia.** *Geoderma* 2018, **332**:60-72.
- 665 11. Peng J, Biswas A, Jiang Q, Zhao R, Hu J, Hu B, Shi Z: **Estimating**  
666 **soil salinity from remote sensing and terrain data in southern**  
667 **Xinjiang Province, China.** *Geoderma* 2019, **337**:1309-1319.
- 668 12. Asghar HN, Setia R, Marschner P: **Community composition and activity**  
669 **of microbes from saline soils and non-saline soils respond**

- 670 similarly to changes in salinity. *Soil Biology and Biochemistry*  
671 2012, **47**:175–178.
- 672 13. Zheng W, Xue D, Li X, Deng Y, Rui J, Feng K, Wang Z-l: The responses  
673 and adaptations of microbial communities to salinity in farmland  
674 soils: a molecular ecological network analysis. *Applied Soil*  
675 *Ecology* 2017, **120**:239–246.
- 676 14. Csonka LN: Physiological and genetic responses of bacteria to  
677 osmotic stress. *Microbiology and Molecular Biology Reviews* 1989,  
678 **53**(1):121–147.
- 679 15. Zhou M-X, Renard M-E, Quinet M, Lutts S: Effect of NaCl on proline  
680 and glycinebetaine metabolism in *Kosteletzkya pentacarpos* exposed  
681 to Cd and Zn toxicities. *Plant and Soil* 2019, **441**(1-2):525–542.
- 682 16. Zhang K, Shi Y, Cui X, Yue P, Li K, Liu X, Tripathi BM, Chu H: Salinity  
683 is a key determinant for soil microbial communities in a desert  
684 ecosystem. *MSystems* 2019, **4**(1).
- 685 17. Yu Y, Zhao C, Zheng N, Jia H, Yao H: Interactive effects of soil  
686 texture and salinity on nitrous oxide emissions following crop  
687 residue amendment. *Geoderma* 2019, **337**:1146–1154.
- 688 18. Ma L, Ma F, Li J, Gu Q, Yang S, Wu D, Feng J, Ding J: Characterizing  
689 and modeling regional-scale variations in soil salinity in the arid  
690 oasis of Tarim Basin, China. *Geoderma* 2017, **305**:1–11.
- 691 19. Khan KS, Mack R, Castillo X, Kaiser M, Joergensen RG: Microbial  
692 biomass, fungal and bacterial residues, and their relationships  
693 to the soil organic matter C/N/P/S ratios. *Geoderma* 2016,  
694 **271**:115–123.
- 695 20. Rath KM, Maheshwari A, Rousk J: The impact of salinity on the  
696 microbial response to drying and rewetting in soil. *Soil Biology*  
697 *and Biochemistry* 2017, **108**:17–26.
- 698 21. Wichern J, Wichern F, Joergensen RG: Impact of salinity on soil  
699 microbial communities and the decomposition of maize in acidic  
700 soils. *Geoderma* 2006, **137**(1-2):100–108.
- 701 22. Yan N, Marschner P, Cao W, Zuo C, Qin W: Influence of salinity and  
702 water content on soil microorganisms. *International Soil and Water*  
703 *Conservation Research* 2015, **3**(4):316–323.
- 704 23. Li X, Sun M, Zhang H, Xu N, Sun G: Use of mulberry-soybean  
705 intercropping in salt-alkali soil impacts the diversity of the soil  
706 bacterial community. *Microb Biotechnol* 2016, **9**(3):293–304.
- 707 24. Chu H, Wang S, Yue H, Lin Q, Hu Y, Li X, Zhou J, Yang Y: Contrasting  
708 soil microbial community functional structures in two major  
709 landscapes of the Tibetan alpine meadow. *MicrobiologyOpen* 2014,  
710 **3**(5):585–594.

- 711 25. Qi Q, Zhao M, Wang S, Ma X, Wang Y, Gao Y, Lin Q, Li X, Gu B, Li  
712 G: **The biogeographic pattern of microbial functional genes along**  
713 **an altitudinal gradient of the Tibetan pasture.** *Frontiers in*  
714 *microbiology* 2017, **8**:976.
- 715 26. Chen FH, Dong GH, Zhang DJ, Liu XY, Jia X, An C-B, Ma MM, Xie YW,  
716 Barton L, Ren X: **Agriculture facilitated permanent human**  
717 **occupation of the Tibetan Plateau after 3600 BP.** *Science* 2015,  
718 **347**(6219):248-250.
- 719 27. Fan R, Short MD, Zeng S-J, Qian G, Li J, Schumann RC, Kawashima N,  
720 Smart RSC, Gerson AR: **The formation of silicate-stabilized**  
721 **passivating layers on pyrite for reduced acid rock drainage.**  
722 *Environmental Science & Technology* 2017, **51**(19):11317-11325.
- 723 28. Nordstrom DK: **Acid rock drainage and climate change.** *Journal of*  
724 *Geochemical Exploration* 2009, **100**(2-3):97-104.
- 725 29. Weatherill JJ, Krause S, Ullah S, Cassidy NJ, Levy A, Drijfhout FP,  
726 Rivett MO: **Revealing chlorinated ethene transformation hotspots**  
727 **in a nitrate-impacted hyporheic zone.** *Water research* 2019,  
728 **161**:222-231.
- 729 30. Bolger AM, Lohse M, Usadel B: **Trimmomatic: a flexible trimmer for**  
730 **Illumina sequence data.** *Bioinformatics* 2014, **30**(15):2114-2120.
- 731 31. Truong DT, Franzosa EA, Tickle TL, Scholz M, Weingart G, Pasolli  
732 E, Tett A, Huttenhower C, Segata N: **MetaPhlan2 for enhanced**  
733 **metagenomic taxonomic profiling.** *Nature methods* 2015,  
734 **12**(10):902-903.
- 735 32. Oksanen J, Kindt R, Legendre P, O'Hara B, Stevens MHH, Oksanen MJ,  
736 Suggests M: **The vegan package.** *Community ecology package* 2007,  
737 **10**(631-637):719.
- 738 33. Goslee SC, Urban DL: **The ecodist package for dissimilarity-based**  
739 **analysis of ecological data.** *Journal of Statistical Software* 2007,  
740 **22**(7):1-19.
- 741 34. Nurk S, Meleshko D, Korobeynikov A, Pevzner PA: **metaSPAdes: a new**  
742 **versatile metagenomic assembler.** *Genome research* 2017,  
743 **27**(5):824-834.
- 744 35. Seemann T: **Prokka: rapid prokaryotic genome annotation.**  
745 *Bioinformatics* 2014, **30**(14):2068-2069.
- 746 36. Li H, Durbin R: **Fast and accurate long-read alignment with**  
747 **Burrows - Wheeler transform.** *Bioinformatics* 2010, **26**(5):589-595.
- 748 37. Khorsandi F, Yazdi FA: **Estimation of Saturated Paste Extracts'**  
749 **Electrical Conductivity from 1:5 Soil/Water Suspension and Gypsum.**  
750 *Communications in Soil Science and Plant Analysis* 2011,  
751 **42**(3):315-321.

- 752 38. Kanso S, Patel BK: **Microvirga subterranea** gen. nov., sp. nov., a  
753 moderate thermophile from a deep subsurface Australian thermal  
754 aquifer. *International journal of systematic and evolutionary*  
755 *microbiology* 2003, **53**(2):401–406.
- 756 39. Martineau C, Mauffrey F, Villemur R: **Comparative analysis of**  
757 **denitrifying activities of Hyphomicrobium nitrativorans,**  
758 **Hyphomicrobium denitrificans, and Hyphomicrobium zavarzinii.**  
759 *Applied and Environmental Microbiology* 2015, **81**(15):5003–5014.
- 760 40. Sauder LA, Albertsen M, Engel K, Schwarz J, Nielsen PH, Wagner M,  
761 Neufeld JD: **Cultivation and characterization of Candidatus**  
762 **Nitrosocosmicus exaquare, an ammonia-oxidizing archaeon from a**  
763 **municipal wastewater treatment system.** *The ISME journal* 2017,  
764 **11**(5):1142–1157.
- 765 41. Shi Y, Delgado-Baquerizo M, Li Y, Yang Y, Zhu Y-G, Peñuelas J, Chu  
766 H: **Abundance of kinless hubs within soil microbial networks are**  
767 **associated with high functional potential in agricultural**  
768 **ecosystems.** *Environment International* 2020, **142**:105869.
- 769 42. Hügler M, Sievert SM: **Beyond the Calvin cycle: autotrophic carbon**  
770 **fixation in the ocean.** *Annual review of marine science* 2011,  
771 **3**:261–289.
- 772 43. Bar-Even A, Noor E, Milo R: **A survey of carbon fixation pathways**  
773 **through a quantitative lens.** *Journal of experimental botany* 2012,  
774 **63**(6):2325–2342.
- 775 44. Crecchio C, Gelsomino A, Ambrosoli R, Minati JL, Ruggiero P:  
776 **Functional and molecular responses of soil microbial communities**  
777 **under differing soil management practices.** *Soil Biology and*  
778 *Biochemistry* 2004, **36**(11):1873–1883.
- 779 45. Tyson GW, Chapman J, Hugenholtz P, Allen EE, Ram RJ, Richardson PM,  
780 Solovyev VV, Rubin EM, Rokhsar DS, Banfield JF: **Community structure**  
781 **and metabolism through reconstruction of microbial genomes from**  
782 **the environment.** *Nature* 2004, **428**(6978):37–43.
- 783 46. Dahl C, Franz B, Hensen D, Kesselheim A, Zigann R: **Sulfite oxidation**  
784 **in the purple sulfur bacterium Allochromatium vinosum:**  
785 **identification of SoeABC as a major player and relevance of SoxYZ**  
786 **in the process.** *Microbiology* 2013, **159**(Pt\_12):2626–2638.
- 787 47. Pott AS, Dahl C: **Sirohaem sulfite reductase and other proteins**  
788 **encoded by genes at the dsr locus of Chromatium vinosum are involved**  
789 **in the oxidation of intracellular sulfur.** *Microbiology* 1998,  
790 **144**(7):1881–1894.
- 791 48. Zhu Y-G, Williams PN, Meharg AA: **Exposure to inorganic arsenic from**  
792 **rice: a global health issue?** *Environmental pollution* 2008,  
793 **154**(2):169–171.

- 794 49. Thoma F: **Light and dark in chromatin repair: repair of UV - induced**  
795 **DNA lesions by photolyase and nucleotide excision repair.** *The EMBO*  
796 *journal* 1999, **18**(23):6585–6598.
- 797 50. Ermolenko D, Makhatadze G: **Bacterial cold-shock proteins.** *Cellular*  
798 *and Molecular Life Sciences CMLS* 2002, **59**(11):1902–1913.
- 799 51. Morgan-Kiss RM, Prisco JC, Pocock T, Gudynaite-Savitch L, Huner NP:  
800 **Adaptation and acclimation of photosynthetic microorganisms to**  
801 **permanently cold environments.** *Microbiology and molecular biology*  
802 *reviews* 2006, **70**(1):222–252.
- 803 52. Fujii DK, Fulco AJ: **Biosynthesis of unsaturated fatty acids by**  
804 **bacilli. Hyperinduction and modulation of desaturase**  
805 **synthesis. [Bacillus megaterium].** *J Biol Chem; (United States)* 1977,  
806 **252**(11).
- 807 53. Zhu K, Choi KH, Schweizer HP, Rock CO, Zhang YM: **Two aerobic pathways**  
808 **for the formation of unsaturated fatty acids in Pseudomonas**  
809 **aeruginosa.** *Molecular microbiology* 2006, **60**(2):260–273.
- 810 54. Chen L-x, Hu M, Huang L-n, Hua Z-s, Kuang J-l, Li S-j, Shu W-s:  
811 **Comparative metagenomic and metatranscriptomic analyses of**  
812 **microbial communities in acid mine drainage.** *The ISME journal* 2015,  
813 **9**(7):1579–1592.
- 814 55. Baker-Austin C, Dopson M: **Life in acid: pH homeostasis in**  
815 **acidophiles.** *Trends in microbiology* 2007, **15**(4):165–171.
- 816 56. Wang M, Chen S, Chen L, Wang D: **Responses of soil microbial**  
817 **communities and their network interactions to saline-alkaline**  
818 **stress in Cd-contaminated soils.** *Environmental Pollution* 2019,  
819 **252**:1609–1621.

820

821

# Figures

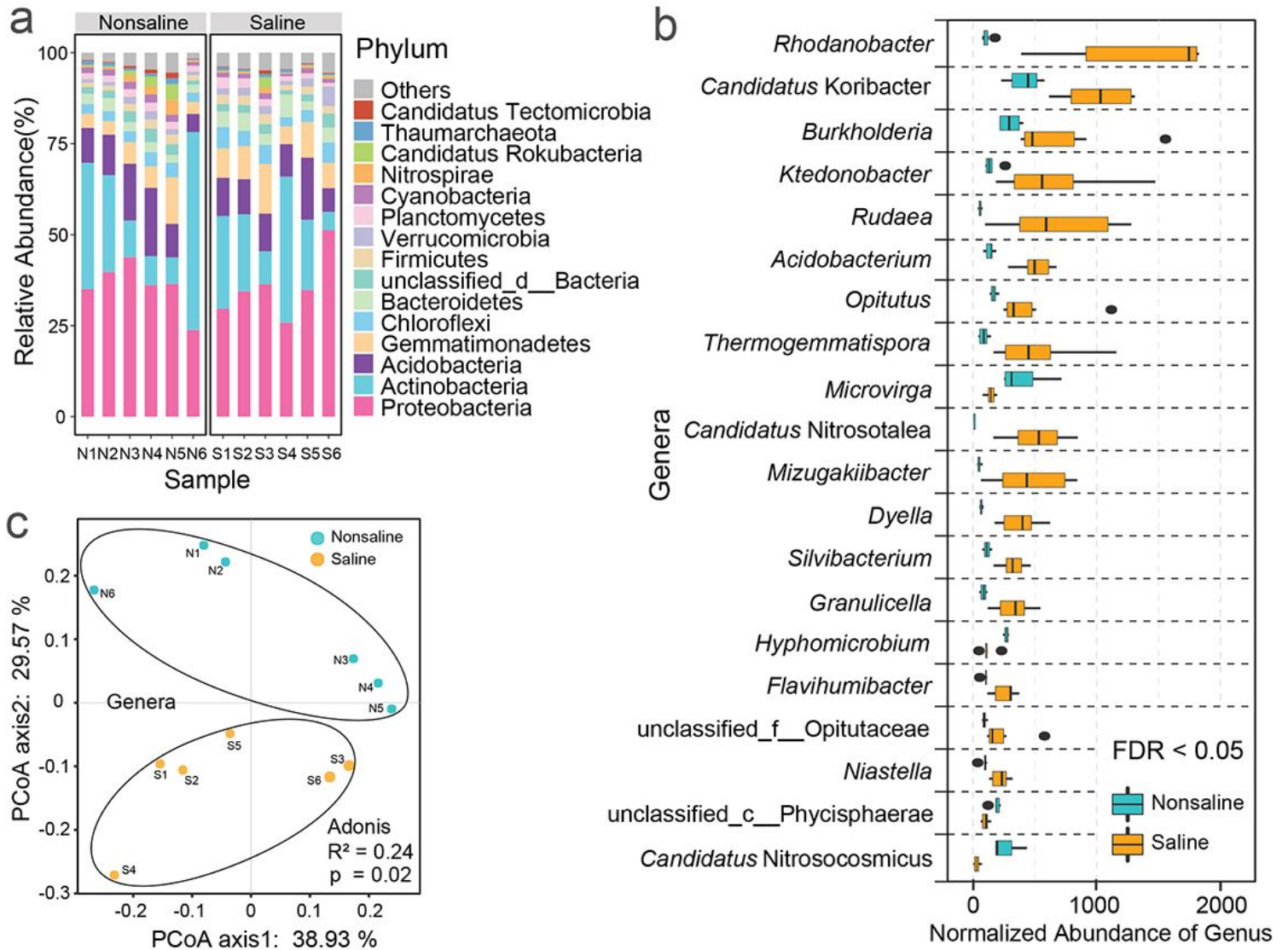


**Figure 1**

Composition and differences in saline and nonsaline soil on the Tibetan Plateau. a. Bacterial composition at the phylum level in saline and nonsaline soil samples of Tibetan Plateau. b. Top 20 genera with significant differences (FDR < 0.05) in saline (orange) and nonsaline (cyan) soil samples of Tibetan Plateau, the total number of reads is normalized to 100000. c. Principal coordinate analysis of saline (orange) and nonsaline (cyan) soil samples based on the composition and abundances of the bacterial communities at the genus level.

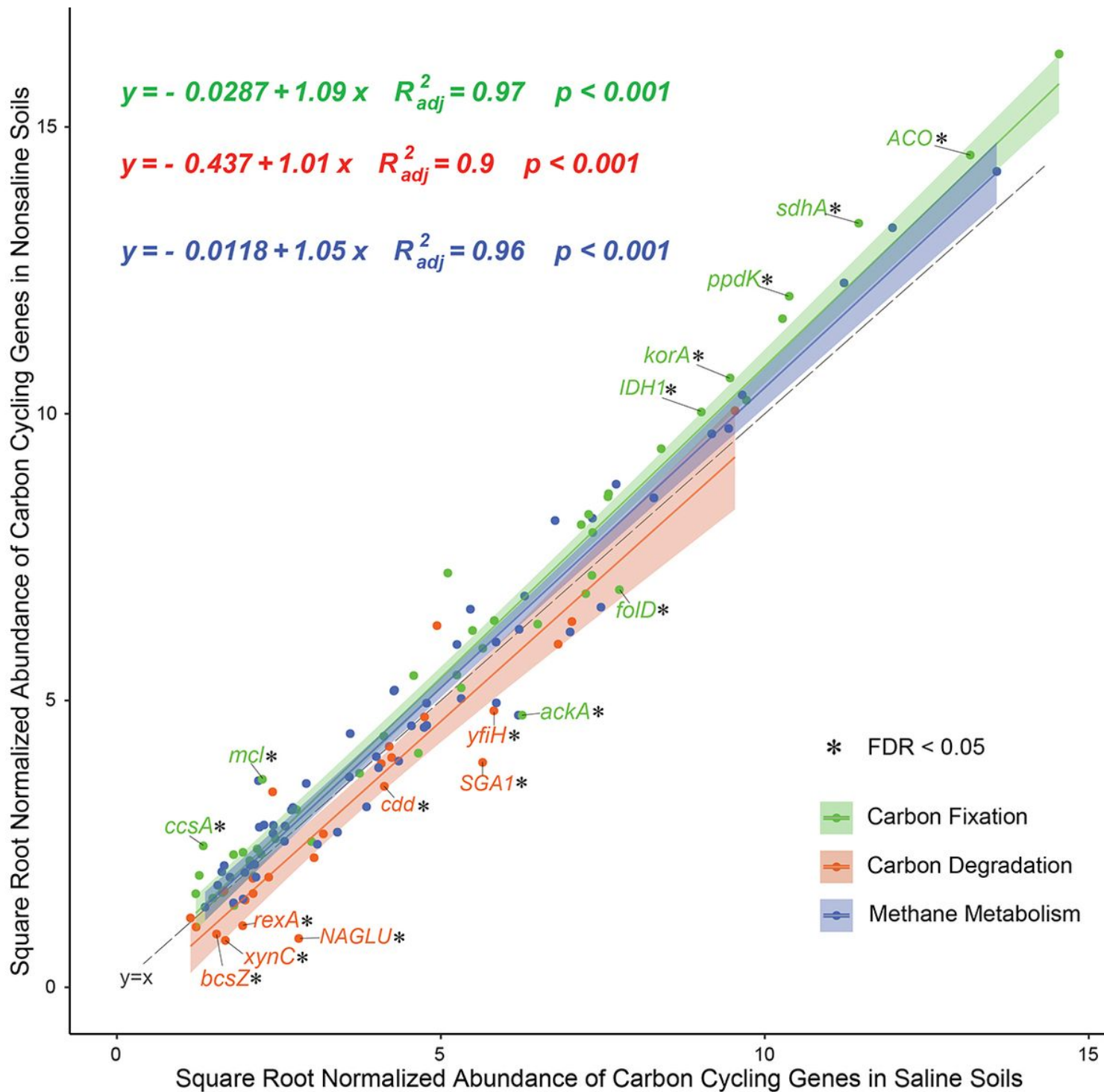


**Figure 2**

The ratio of genes in carbon cycling pathway in saline and nonsaline soil on the Tibetan Plateau. The black dotted line equation “y = x” indicates that the horizontal and vertical axes are equal. Green, red, and blue represent genes of carbon fixation, carbon degradation, and methane metabolism pathways, respectively. Genes with significant differences (FDR < 0.05) are marked in the corresponding colors and connected with short lines. The total number of reads is normalized to 100000.

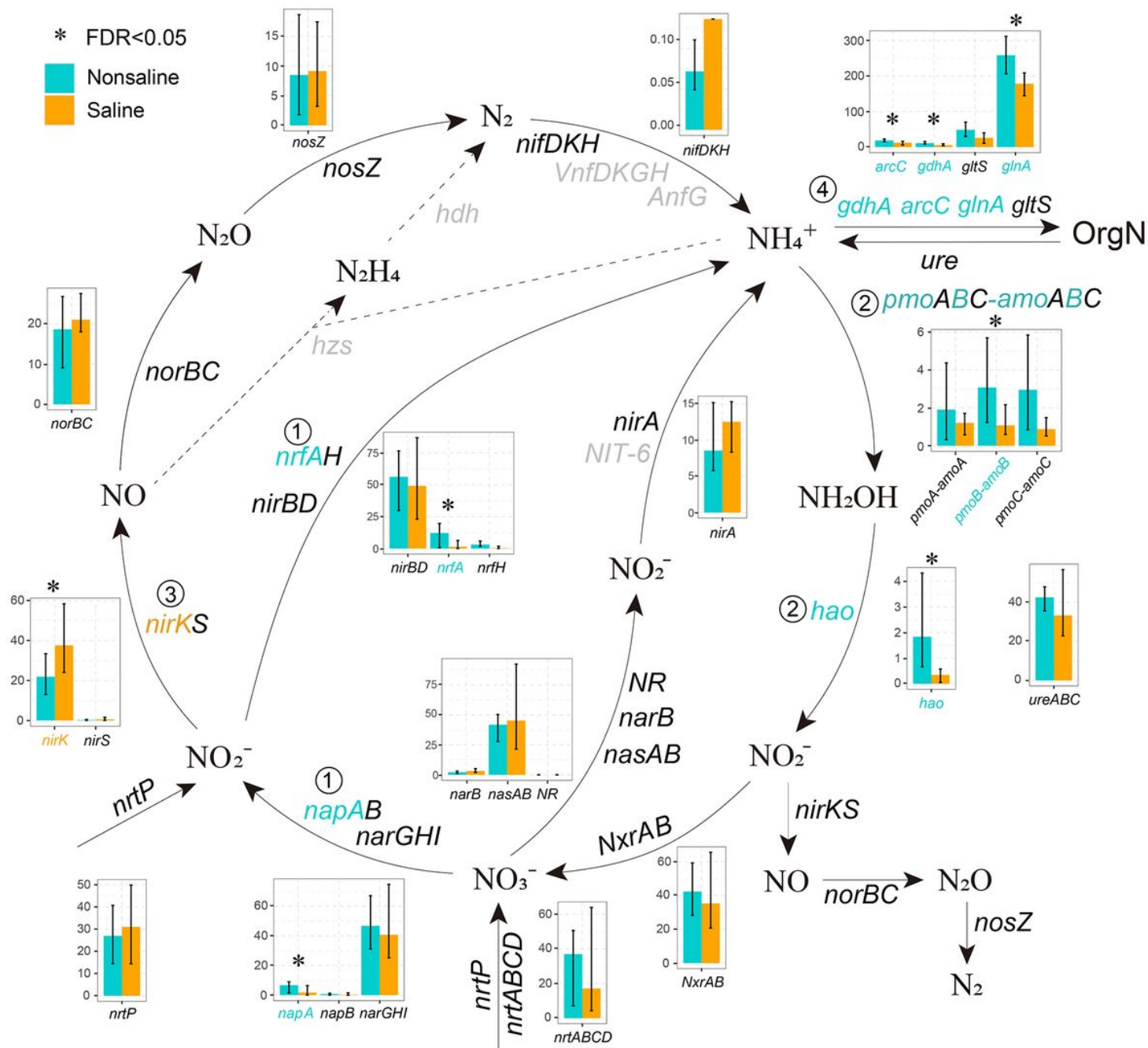


**Figure 3**

Differences in the abundance of genes related to nitrogen cycling in the saline (orange) and nonsaline (cyan) soil on the Tibetan Plateau. Bar plots show the normalized abundances of nitrogen cycling genes. Significantly different (FDR < 0.05) genes are marked with “\*” and circled numbers. Undetected genes are indicated in gray. Circled numbers identify genes with significant differences: 1, dissimilatory nitrate reduction; 2, nitrification; 3, denitrification; and 4, organic nitrogen conversion. The total number of reads is normalized to 100000.

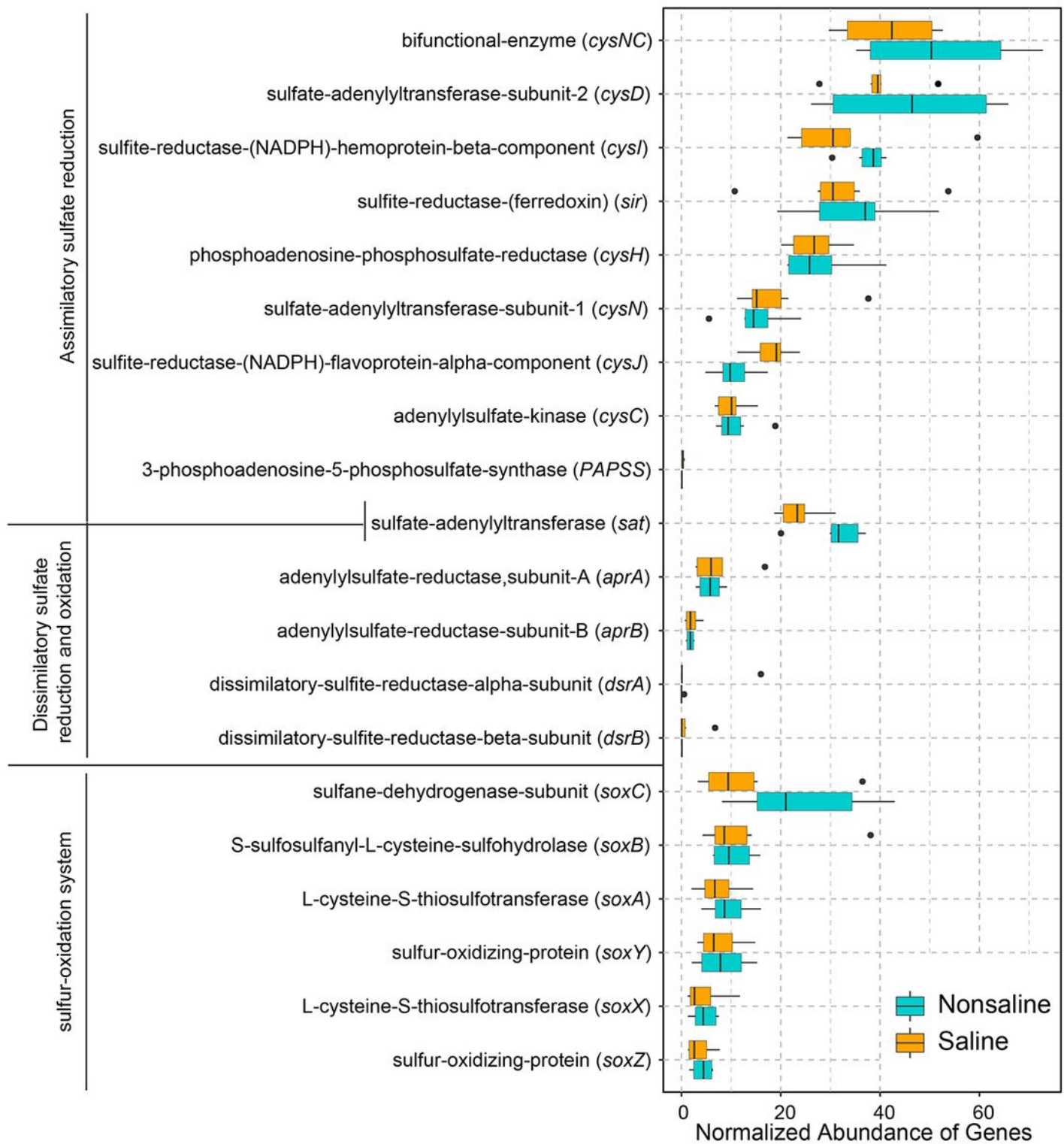


**Figure 4**

Difference in abundances of sulfur cycling genes in saline (orange) and nonsaline (cyan) soil on the Tibetan Plateau. The total number of reads is normalized to 100000.

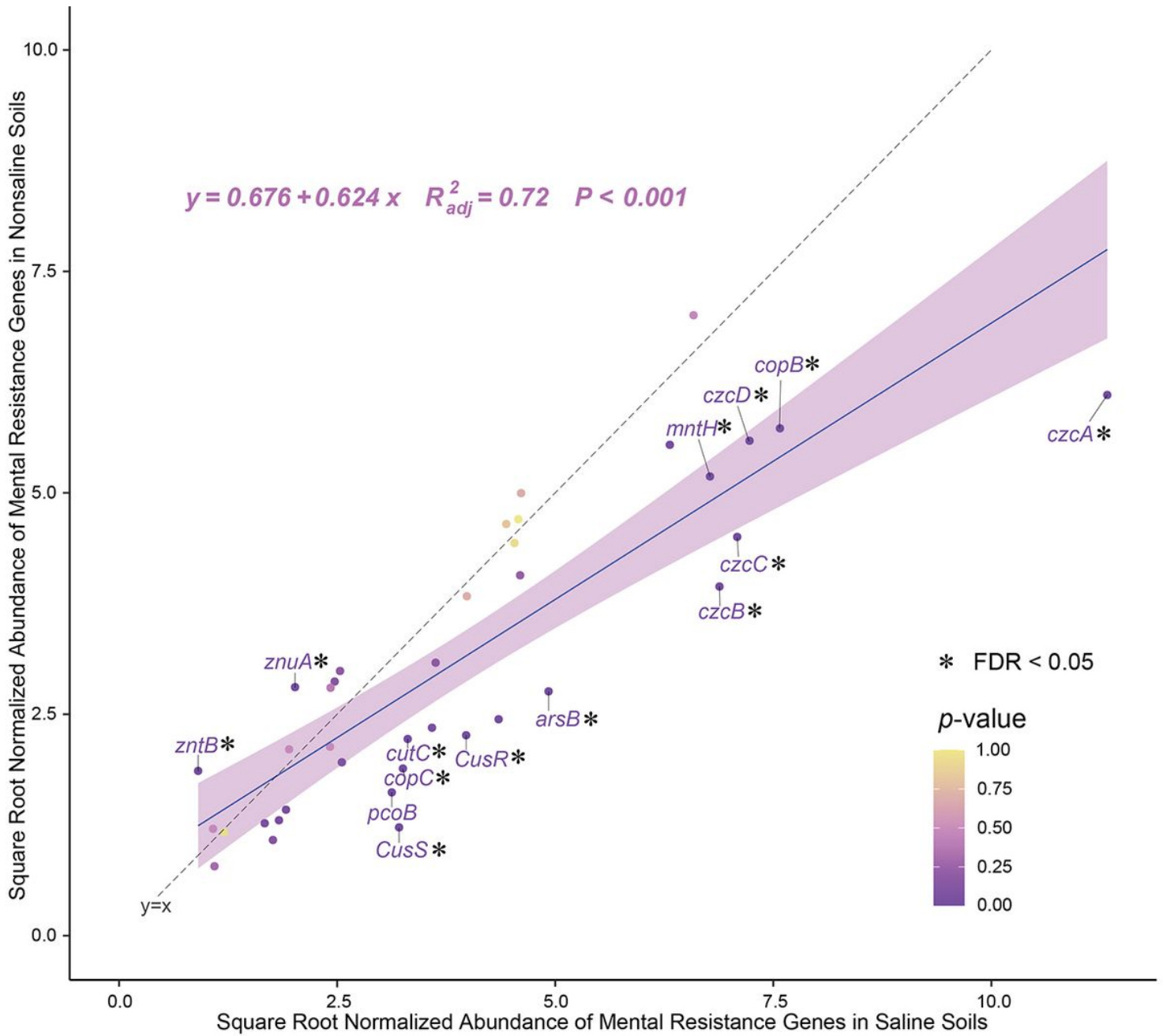


**Figure 5**

Abundance of heavy metal(loid) resistance genes in saline and nonsaline soil on the Tibetan Plateau. The black dotted line with the equation “y = x” indicates that the horizontal and vertical axes are equal. Genes with significantly different abundances (FDR < 0.05) are marked in purple and connected with short lines. The total number of reads is normalized to 100000.

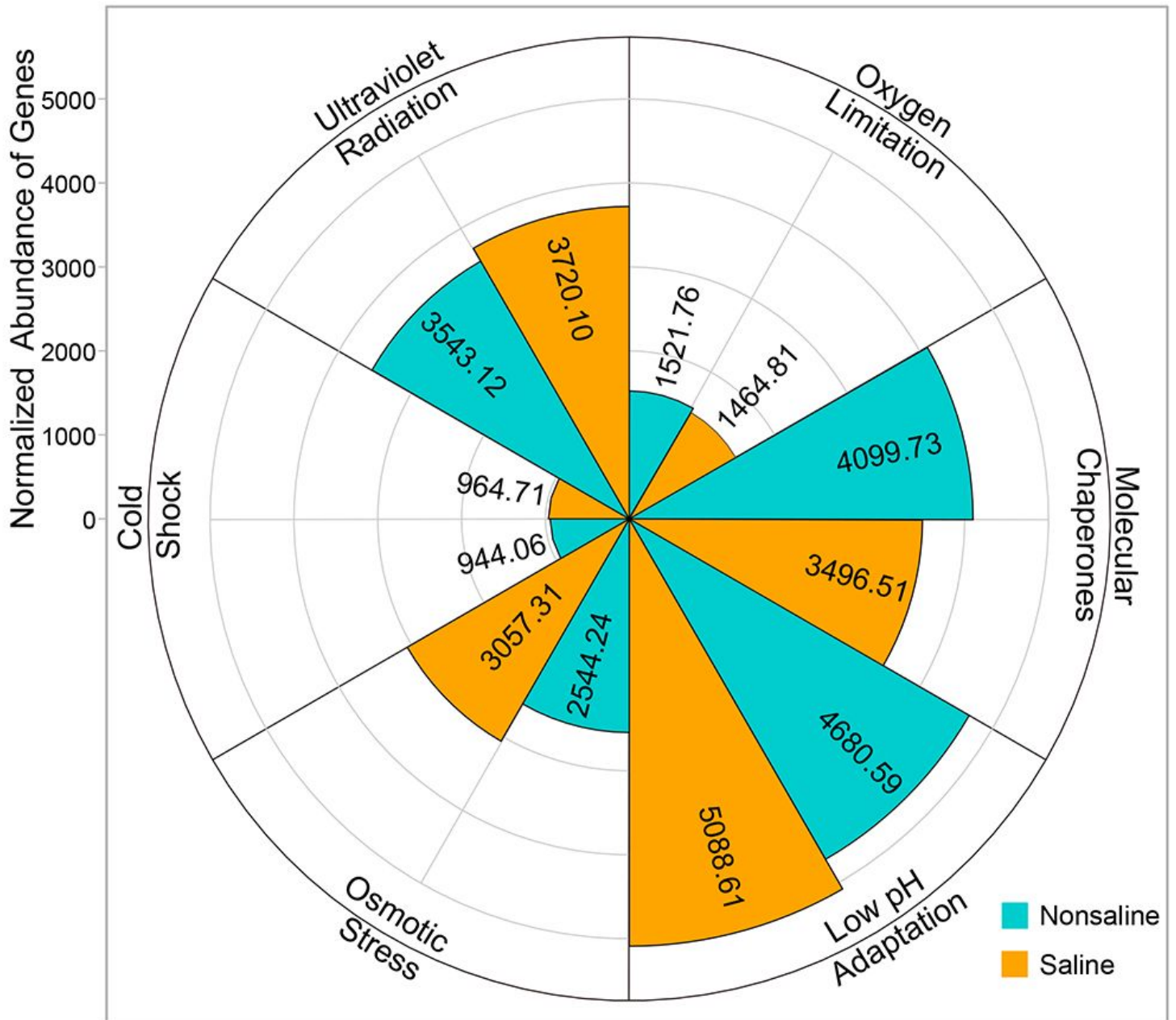


**Figure 6**

Abundance of the environmental stress resistance genes. The total number of reads is normalized to 100000.

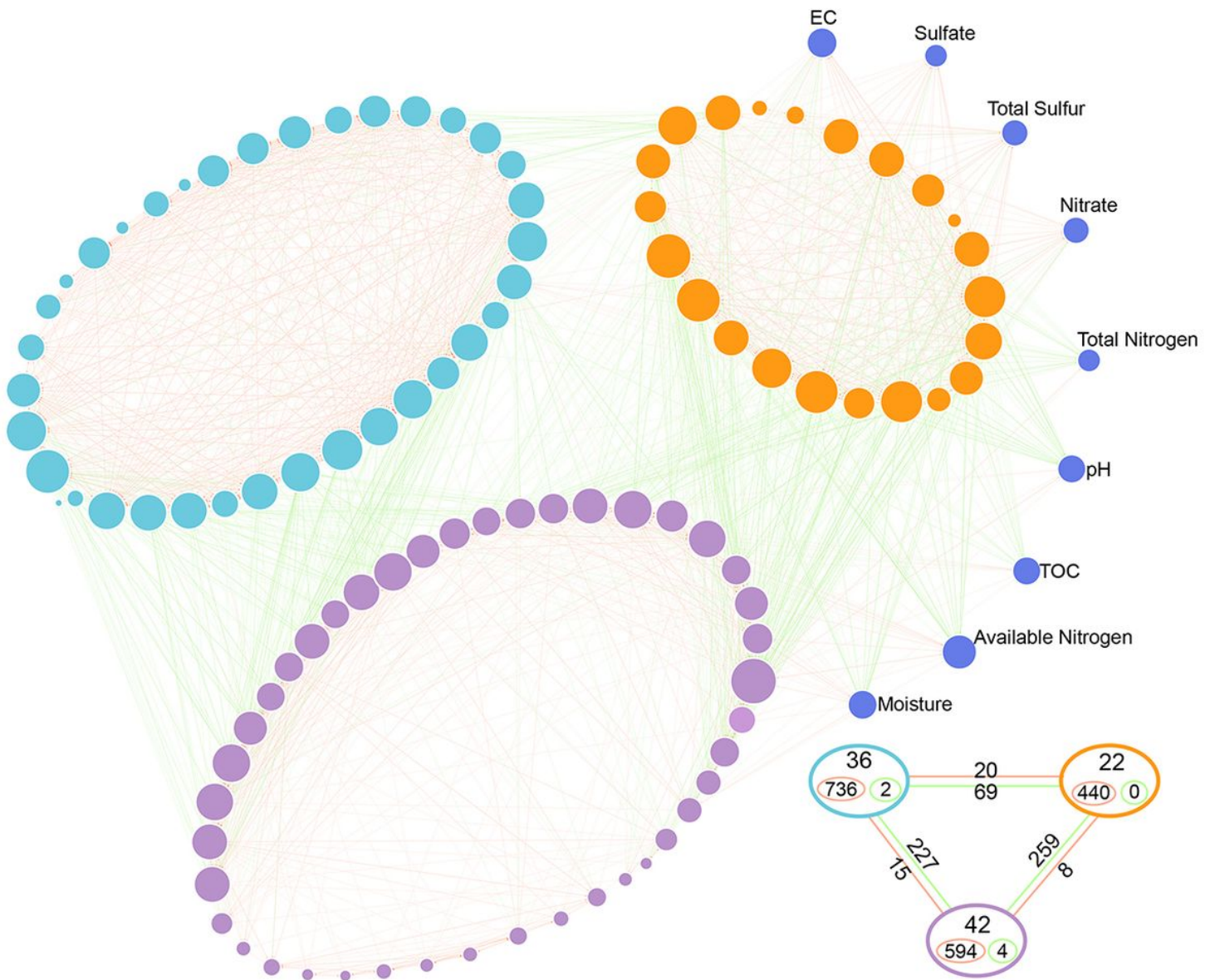


**Figure 7**

Network of the top 100 dominant genera and physicochemical parameters. A connection denotes a Spearman's correlation coefficient with a magnitude greater than 0.6 (positive correlation = red lines) or less than  $-0.6$  (negative correlation = green lines) and statistically significant ( $p$ -value  $< 0.05$ ). The size of each node is proportional to the number of connections (i.e., degree). The thickness of each connection between two nodes (i.e., edge) is proportional to the Spearman's correlation coefficient (i.e., weight), ranging from  $|0.6|$  to  $|1|$ . The network is colored according to the modules, where the nodes clustered in the same module share the same color. The lower right corner is a schematic diagram, and the large circles represent three modules based on network analysis, and the positions are corresponding. In the large circles, the top number indicates the number of nodes, the red circle and the number indicate positive correlation within the module, and the green indicates negative correlation. Between the large circles, red lines and numbers indicate positive correlations, and green lines and numbers indicate negative correlations.

## Supplementary Files

This is a list of supplementary files associated with this preprint. Click to download.

- [supplementary1.docx](#)